Current Research in Toxicology 2 (2021) 341–356

Contents lists available at ScienceDirect

Current Research in Toxicology

journal homepage: www.elsevier.com/locate/crtox

Sex-specific acute and chronic neurotoxicity of acute diisopropylfluorophosphate (DFP)-intoxication in juvenile Sprague-Dawley rats

Eduardo A. González [a], Jonas J. Calsbeek [a], Yi-Hua Tsai [a], Mei-Yun Tang [a], Peter Andrew [a], Joan Vu [a], Elizabeth L. Berg [b], Naomi H. Saito [c], Danielle J. Harvey [c], Suangsuda Supasai [a,1], Gene G. Gurkoff [d,e], Jill L. Silverman [b,f], Pamela J. Lein [a,f,*]

[a] Department of Molecular Biosciences, University of California, Davis, School of Veterinary Medicine, 1089 Veterinary Medicine Drive, Davis, CA 95616, USA
[b] Department of Psychiatry, University of California, Davis, School of Medicine, 2230, Stockton Boulevard, Sacramento, CA 95817, USA
[c] Department of Public Health Sciences, University of California, Davis, One Shields Avenue, School of Medicine, Davis, CA 95616, USA
[d] Department of Neurological Surgery, University of California, Davis, School of Medicine, 4860 Y Street, Sacramento, CA 95817, USA
[e] Center for Neuroscience, University of California, Davis, 1544 Newton Court, Davis, CA 95618, USA
[f] MIND Institute, University of California, Davis, 2825 50th Street, Sacramento, CA 95817, USA

ARTICLE INFO

Keywords:
Cognitive deficits
Neurodegeneration
Neurogenesis
Neuroinflammation
Seizures
Sex differences

ABSTRACT

Preclinical efforts to improve medical countermeasures against organophosphate (OP) chemical threat agents have largely focused on adult male models. However, age and sex have been shown to influence the neurotoxicity of repeated low-level OP exposure. Therefore, to determine the influence of sex and age on outcomes associated with acute OP intoxication, postnatal day 28 Sprague-Dawley male and female rats were exposed to the OP diisopropylfluorophosphate (DFP; 3.4 mg/kg, s.c.) or an equal volume of vehicle (~80 μL saline, s.c.) followed by atropine sulfate (0.1 mg/kg, i.m.) and pralidoxime (2-PAM; 25 mg/kg, i.m.). Seizure activity was assessed during the first 4 h post-exposure using behavioral criteria and electroencephalographic (EEG) recordings. At 1 d post-exposure, acetylcholinesterase (AChE) activity was measured in cortical tissue, and at 1, 7, and 28 d post-exposure, brains were collected for neuropathologic analyses. At 1 month post-DFP, animals were analyzed for motor ability, learning and memory, and hippocampal neurogenesis. Acute DFP intoxication triggered more severe seizure behavior in males than females, which was supported by EEG recordings. DFP caused significant neurodegeneration and persistent microglial activation in numerous brain regions of both sexes, but astrogliosis occurred earlier and was more severe in males compared to females. DFP males and females exhibited pronounced memory deficits relative to sex-matched controls. In contrast, acute DFP intoxication altered hippocampal neurogenesis in males, but not females. These findings demonstrate that acute DFP intoxication triggers seizures in juvenile rats of both sexes, but the seizure severity varies by sex. Some, but not all, chronic neurotoxic outcomes also varied by sex. The spatiotemporal patterns of neurological damage suggest that microglial activation may be a more important factor than astrogliosis or altered neurogenesis in the pathogenesis of cognitive deficits in juvenile rats acutely intoxicated with OPs.

Abbreviations: AChE, acetylcholinesterase; AS, atropine-sulfate; BChE, butyrylcholinesterase; ChE, cholinesterase; CT, computed tomography; DFP, diisopropylfluorophosphate; EEG, electroencephalogram; FJC, Fluoro-Jade C; i.m., intramuscular; i.p., intraperitoneal; OP, organophosphate; 2-PAM, pralidoxime; PBS, phosphate-buffered saline; ROI, region of interest; s.c., subcutaneous; SE, status epilepticus; T2w, T2-weighted; VEH, vehicle.

* Corresponding author at: Department of Molecular Biosciences, University of California, Davis, School of Veterinary Medicine, 1089 Veterinary Medicine Drive, 2009 VM3B, Davis, CA 95616, USA.

E-mail addresses: azgonzalez@ucdavis.edu (E.A. González), jcalsbeek@ucdavis.edu (J.J. Calsbeek), yihtsai@ucdavis.edu (Y.-H. Tsai), mytang@ucdavis.edu (M.-Y. Tang), pandrew@ucdavis.edu (P. Andrew), jopvu@ucdavis.edu (J. Vu), lizberg@ucdavis.edu (E.L. Berg), nhsaito@ucdavis.edu (N.H. Saito), djharvey@ucdavis.edu (D.J. Harvey), ssupasai@ucdavis.edu (S. Supasai), gggurkoff@ucdavis.edu (G.G. Gurkoff), jsilverman@ucdavis.edu (J.L. Silverman), pjlein@ucdavis.edu (P.J. Lein).

[1] Present address: Department of Molecular Tropical Medicine and Genetics, Faculty of Tropical Medicine, Mahidol University, Bangkok 10400, Thailand.

https://doi.org/10.1016/j.crtox.2021.09.002
Received 8 July 2021; Revised 6 September 2021; Accepted 9 September 2021
Available online xxxx

1. Introduction

Organophosphorus cholinesterase inhibitors (OPs) are widely used pesticides that cause hundreds of thousands of deaths each year as a result of accidental and intentional poisonings (Pereira et al., 2014; Mew et al., 2017). OPs have also been weaponized for use against military and civilian targets, as evidenced by the 2017 chemical attacks in Syria (UN, 2017), as well as the assassination attempts of a former intelligence agent in 2018 (Haley, 2018) and a Russian opposition leader in 2020 (OPCW, 2020). Acute OP intoxication can trigger seizures that rapidly progress to *status epilepticus* (SE) and ultimately death (Pope and Brimijoin, 2018). Current medical countermeasures for OP-induced cholinergic crisis include atropine to block excessive cholinergic signaling via muscarinic receptors, benzodiazepines to terminate seizures, and pralidoxime (2-PAM) to reactivate AChE (Jett et al., 2020). These therapeutics must be administered within minutes after SE initiation to be maximally effective (Jett and Spriggs, 2020), but even then, they do not adequately protect against the long-term neurological deficits observed in survivors, including structural brain damage and persistent cognitive deficits (Figueiredo et al., 2018; Jett et al., 2020). There is, therefore, an urgent need to identify more effective medical countermeasures for treating individuals acutely intoxicated with OPs.

In the event of a civilian mass casualty involving OPs, it is likely that a diverse population varying in age and sex will be affected. However, current preclinical research to develop improved medical countermeasures has almost exclusively used adult male models. This is a troubling gap given an extensive literature indicating that children are more susceptible than adults to the neurotoxic effects of environmentally relevant OP levels (Muñoz-Quezada et al., 2013; González-Alzaga et al., 2014; Sagiv et al., 2019), and that neurotoxic outcomes of repeated low-level OP exposures can be sex-specific (Rauh et al., 2012; Comfort and Re, 2017). A recent preclinical study demonstrated that rats at varying stages of neurodevelopment are differentially susceptible to the proconvulsant activity of OP chemical threat agents, and postnatal day (PND) 28 was found to be the youngest age at which OPs consistently elicited seizures (Scholl et al., 2018). While both sexes were included in this earlier study, sex-specific effects were not directly addressed, and no long-term outcomes were evaluated. Therefore, we sought to determine whether acute OP intoxication during early-life brain development has neurological consequences, and if so, whether sex differences were identifiable.

Diisopropylfluorophosphate (DFP), which is considered an OP chemical threat agent by the United States Department of Homeland Security (Jett and Spriggs, 2020), can induce acute seizures as well as long-term neurological deficits in adult rodent models (Pessah et al., 2016; Putra et al., 2019; Guignet et al., 2020). Acute DFP intoxication also is associated with a significant neuroinflammatory response in adult animals (Hobson et al., 2019; Guignet et al., 2020; Rojas et al., 2020). Therefore, the goal of this study was to develop and characterize a juvenile model of acute DFP intoxication to evaluate seizure responses and persistent neurological consequences in male vs. female rats.

2. Materials and methods

2.1. Animal husbandry

All animal studies adhered strictly to the ARRIVE guidelines and the National Institutes of Health guide for the care and use of laboratory animals (NIH publication No. 8023, revised 1978), and were conducted in accordance with a protocol approved by the UC Davis Institutional Animal Care and Use Committee (IACUC, protocol #21954) designed to minimize pain and suffering. All animals in this study were maintained in facilities fully accredited by AAALAC International. Juvenile male and female Sprague-Dawley rats born to timed-pregnant dams (Charles River Laboratories, Hollister, CA, USA) were weaned at PND 21, at which time they were separated by sex with two animals of the same sex per cage. Animals were housed in standard plastic shoebox cages in an environmentally controlled vivarium (22 ± 2 °C, 40–50% humidity, 12 h light/dark cycle). Food (2018 Teklad global 18% protein rodent diet; Envigo, Huntingdon, UK) and water were provided *ad libitum*.

2.2. DFP exposure paradigm

A dose range finding study was conducted in PND 28 male and female rats using the up-and-down dosing procedure (Bruce, 1985) to identify a dose of DFP that caused ≤ 20% mortality. A starting dose of 6 mg/kg DFP was selected because this dose had been reported to induce seizure activity in juvenile PND 28 rats (Scholl et al., 2018). The following doses were tested in both sexes: 1.9, 3.4, 6, and 19 mg/kg. A dose of 1.1 mg/kg was also tested in females, but not males because DFP at 1.9 mg/kg had no effect on survival or seizure behavior in males.

DFP (Sigma Chemical Company, St. Louis, MO, USA) was prepared in ice-cold sterile phosphate-buffered saline (PBS, 3.6 mM Na_2HPO_4, 1.4 mM NaH_2PO_4, 150 mM NaCl; pH 7.2) within 5 min of injection (s.c.). DFP purity was evaluated using previously described ^{1}H, ^{13}C, ^{19}F and ^{31}P NMR methods (Gao et al., 2016) and found to be approximately 90 ± 7% pure. Upon receipt in the laboratory, DFP was aliquoted and stored at –80 °C, a condition under which it retains stability for over 1 year (Heiss et al., 2016). Vehicle (VEH) controls were administered a similar volume (~80 μL) of sterile PBS in place of DFP. One min after DFP or VEH injection, all animals were administered a combined injection (i.m.) of atropine-sulfate (AS, 0.1 mg/kg; Sigma; >97% purity) and pralidoxime (2-PAM, 25 mg/kg; Sigma; >99% purity). Both compounds increase survival by protecting against peripheral cholinergic toxicity (Pessah et al., 2016). Animals were randomly assigned to groups using a random number generator.

Following DFP or VEH injection, animals were monitored for seizure behavior for 4 h (Fig. 1**A**) as previously described (Guignet et al., 2020) using a previously published scale of seizure behavior severity (Deshpande et al., 2010). At the end of the observation period, all subjects were injected (s.c.) with 3 mL of 10% w/v dextrose in sterile saline to replace fluids lost due to cholinergic crisis, and then returned to their home cages. Rat food was softened with H_2O until animals were able to resume consumption of solid food, typically within 2–3 d. Subjects were anesthetized using 1–3% isoflurane (MWI Animal Health, Boise, ID, USA) in medical grade oxygen (flow rate = 1 L/min) at 1, 7, or 28 d post-intoxication and euthanized by exsanguination to collect brain tissue for further analyses (Fig. 1**A**).

2.3. Electroencephalography (EEG)

A separate cohort of animals not used for biochemical, histological, or behavioral analyses was implanted with cortical electrodes and monitored for EEG activity for ~ 2 h post-DFP to confirm seizure activity. EEG implantations and recordings were performed as previously described (González et al., 2020). Briefly, PND 22 animals were deeply anesthetized with 1–3% isoflurane (MWI Animal Health) in medical grade oxygen (flow rate = 1 L/min). Animals were secured in a stereotaxic platform (Stoelting, Wood Dale, IL, USA), the surgical site was thoroughly cleaned using a betadine scrub (Purdue Products, Stamford, CT, USA) and 70% isopropyl alcohol wipes (Covidien Plc, Dublin, Ireland), and a 1-inch incision made along the top of the skull. Four stainless steel head mount screws (P1 Technologies, Roanoke, VA, USA) were implanted into the skull and connected to sterile HD-X02 telemetry devices (Data Sciences International, St. Paul, MN, USA) that were inserted between the skin and muscle layer along the flank of the

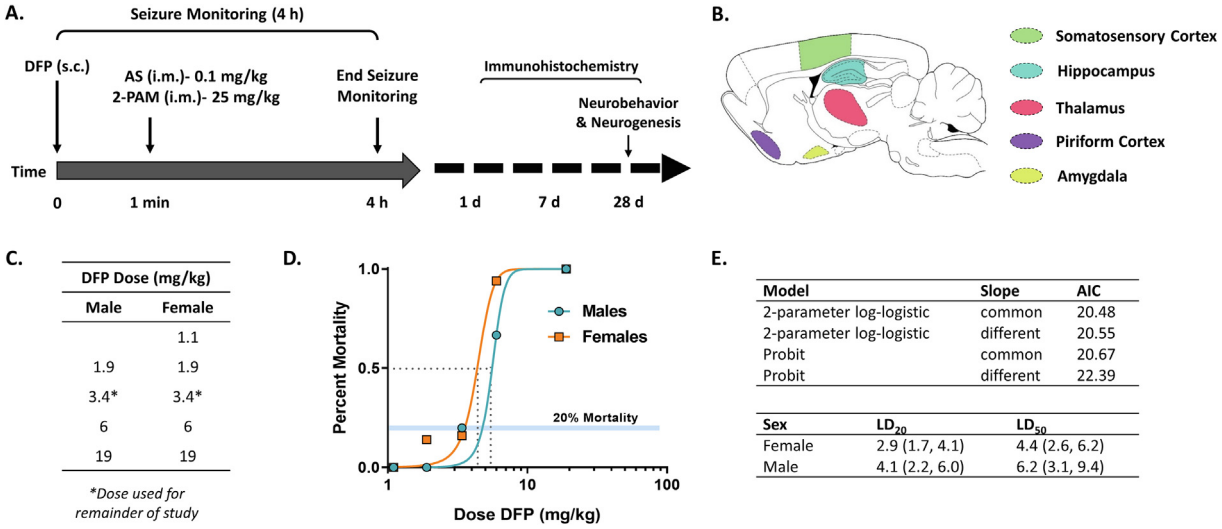

Fig. 1. DFP exposure paradigm and dose–response assessment. (**A**) Schematic illustrating the dosing paradigm used to intoxicate juvenile male and female PND 28 Sprague Dawley rats and times post-exposure when other data points were collected. (**B**) Illustration of the five brain regions examined for neuropathology following acute DFP intoxication. (**C**) DFP doses tested and (**D**) mortality dose–response curve using varying doses of DFP. Based on these data, 3.4 mg/kg was selected for all subsequent studies. Sample sizes range from 3 to 4 at the end doses (1.1, 1.9, and 19 mg/kg) and 6–10 at the middle doses (3.4 and 6 mg/kg). (**E**) Statistical models tested for dose–response analysis. Model with the smallest Akaike Information Criterion (AIC) is the strongest statistical model. Estimated LD_{20} and LD_{50} values by sex (95% confidence interval are included in parentheses). No significant difference between sexes was observed.

animal. A second 1-inch incision was made along the anterior flank to enable telemeter insertion. The incision was sutured (Ethicon, Bridgewater, NJ, USA) and animals were allowed to recover for 6 d before being exposed to DFP at PND 28.

On the day of recordings, animals were placed on PhysioTel Receivers (Data Sciences International) and baseline EEG activity was recorded for ~ 1 h (Ponemah software, Data Sciences International). Animals were then injected with DFP (3.4 mg/kg, s.c) and recorded for ~ 2 h post-injection. EEG traces were analyzed using NeuroScore software (Data Sciences International) and a band-pass filter of 20–70 Hz for noise reduction as previously described (Pouliot et al., 2016). Root mean squared (RMS) values were automatically extracted from the filtered traces using epochs of 1 s and used to quantify spike amplitude. Spikes in the data that reached > 2x baseline were extracted to quantify spike frequency (# spikes/s above baseline). Each of these quantified metrics were averaged over a 1 h baseline recording (pre-DFP) and a 2 h seizure period (post-DFP).

2.4. Cholinesterase activity assays

Following euthanasia, brains were immediately removed, bisected sagittally, and the left hemisphere dissected on ice to remove the cortex. We previously showed that cholinesterase activity in the cortex is representative of cholinesterase activity in multiple major brain regions following acute DFP intoxication in adult rats (González et al., 2020). The cortical tissue was snap frozen on dry ice and stored at −80 °C until analyzed. The Ellman assay (Ellman et al., 1961) was used to measure total cholinesterase (ChE), acetylcholinesterase (AChE), and butyrylcholinesterase (BChE) activity as previously described (González et al., 2020). Briefly, samples were homogenized in lysis buffer (0.1 M phosphate buffer, pH 8.0 with 0.1% w/v Triton X-100) and centrifuged for 1 min (13,400 × g) at 4 °C. Supernatant was collected, and triplicate samples of each supernatant transferred to a 96-well plate. Samples were equilibrated for 5 min with the colorimetric reagent 5,5′-dithio-bis(2-nitrobenzoicacid) (Sigma), and then allowed to react with the AChE substrate acetylthiocholine iodide (Sigma). Enzyme activity was quantified by measuring changes in absorbance at 405 nm over 15 min. All samples were run in the absence or presence of 100 μM of the BChE inhibitor, tetraisopropyl pyrophosphoramide (Sigma), to determine total ChE and AChE activity, respectively. BChE activity was calculated by subtracting AChE activity from total ChE activity in each sample. Enzyme activity of each sample was normalized by total protein concentration of that sample, as determined using the BCA assay (Pierce, Rockford, IL, USA).

2.5. Neuropathologic analyses

The remaining right hemisphere was blocked into 2 mm thick sections using a stainless-steel small rat brain matrix (Kent Scientific, Torrington, CT, USA) and post-fixed in cold 4% w/v paraformaldehyde (Sigma) in PBS (pH 7.2) for 24 h at 4 °C. Tissue sections were then incubated overnight in 30% w/v sucrose (Thermo Fisher, Waltham, MA, USA) in PBS at 4 °C and subsequently embedded in OCT medium (Thermo Fisher) and stored at −80 °C until processing. All brain sections were cryosectioned at −20 °C into 10 μm slices on Superfrost Plus slides (Thermo Fisher). Each endpoint was examined in five brain regions using a minimum of 2 slides per region as previously described (Guignet et al., 2020): somatosensory cortex, hippocampus (including the CA1, CA3, and dentate gyrus subregions), thalamus, piriform cortex, and amygdala (Fig. 1**B**). All endpoints were assessed in sequential 10 μm thick brain sections.

Fluoro-Jade C (FJC) staining was performed as previously described (Supasai et al., 2020). Briefly, brain sections were stained using 0.06% w/v potassium permanganate (Sigma) in distilled water, washed in distilled water, and incubated for 10 min in 0.0001% w/v FJC (Cat #AG325; Millipore, Billerica, MA, USA) in 0.017 M acetic acid (Acros Organics, Geel, Belgium) in distilled water. DAPI solution (0.1 μg/mL in water; Invitrogen, Carlsbad, CA, USA) was also included to label all cell nuclei. Slides were then cleared in chemical grade xylene (Thermo Fisher) and mounted in 50 μL of Permount (Thermo Fisher).

Immunohistochemistry experiments were performed as previously described (Supasai et al., 2020). All primary and secondary antibodies used in this study are listed in Table 1. Briefly, antigen retrieval was performed using 10 mM citrate buffer (pH 6.0) in distilled water at 90 °C for 20 min. To block nonspecific binding, slides were incubated in a blocking buffer comprised of 10% v/v normal goat serum (Vector Laboratories, Burlingame, CA, USA), 1% w/v bovine serum albumin (Sigma), and 0.03% w/v Triton X-100 (Thermo Fisher) in PBS for

Table 1
Primary and secondary antibodies used in this study.

Primary Antibodies				
	Antibody	Dilution	RRID	Source
IBA-1	Rabbit anti-ionized calcium-binding adapter molecule 1	1:1000	RRID:AB_839504	Wako Laboratory Chemicals (Richmond, VA)
CD68	Mouse anti-CD68	1:200	RRID:AB_2291300	Serotec (Hercules, CA)
GFAP	Mouse anti-glial fibrillary acidic protein	1:1000	RRID:AB_561049	Cell Signaling Technologies (Danvers, MA)
S100β	Rabbit anti-S100 calcium-binding protein β	1:500	RRID:AB_2184443	Abcam (Cambridge, UK)
DCX	Guinea pig anti-doublecortin	1:500	RRID:AB_1586992	Millipore (Billerica, MA)
Ki67	Rabbit anti-ki67	1:750	RRID:AB_2756822	Abcam (Cambridge, UK)
NeuN	Mouse anti-neuronal nuclei	1:500	RRID:AB_2298772	Millipore (Billerica, MA)
Secondary Antibodies				
	Antibody	**Dilution**	**RRID**	**Source**
IBA-1	Alexa Fluor 568-conjugated goat anti-rabbit IgG	1:500	RRID:AB_2535730	Life Technologies (Carlsbad, CA)
CD68	Alexa Fluor 488-conjugated goat anti-mouse IgG	1:500	RRID:AB_2534069	Life Technologies (Carlsbad, CA)
GFAP	Alexa Fluor 568-conjugated goat anti-mouse IgG1	1:1000	RRID:AB_2535766	Life Technologies (Carlsbad, CA)
S100β	Alexa Fluor 488-conjugated goat anti-rabbit IgG	1:500	RRID:AB_2576217	Life Technologies (Carlsbad, CA)
DCX	Alexa-Fluor 594-conjugated goat anti-guinea pig IgG	1:1000	RRID:AB_2534120	Life Technologies (Carlsbad, CA)
Ki67	Alexa-Fluor 488-conjugated goat anti-rabbit IgG	1:500	RRID:AB_2576217	Life Technologies (Carlsbad, CA)
NeuN	Alexa-Fluor 647-conjugated goat anti-mouse IgG	1:500	RRID:AB_2535809	Life Technologies (Carlsbad, CA)

1 h at room temperature. Following blocking, slides were incubated overnight at 4 °C with primary antibodies in blocking buffer. Negative controls incubated in blocking buffer in place of a primary antibody were included in each staining batch.

Following primary antibody incubation, slides were washed 3 times in PBS with 0.03% w/v Triton X-100 for 10 min each and subsequently incubated in secondary antibody solution for 90 min at room temperature in the dark. Following incubation, slides were rinsed 3 times in PBS with 0.03% w/v Triton X-100 for 10 min each and cover slipped in 50 μL ProLong Gold Antifade Mountant with DAPI (Invitrogen).

Slides were scanned at 20X magnification using a high-content ImageXpress XL imaging system (Molecular Devices, Sunnyvale, CA, USA). Regions of interest (ROI) were created for the amygdala, piriform cortex, somatosensory cortex, and hippocampus, including the CA1, CA3, and dentate gyrus subregions, between −3.6 mm to −4.2 mm posterior to bregma, as well as the thalamus between −3.0 mm to −3.6 mm posterior to bregma. Bregma ranges were confirmed using a rat brain atlas (Kruger et al., 1995). Fluorescent images were quantified as previously described (Supasai et al., 2020). The percent area of positive fluorescence was quantified for each marker and normalized to the total area analyzed, which was held constant across all animals. Positive staining was defined as fluorescence that reached ≥ 2x background fluorescence intensity observed in negative control images. Percent area of immunostaining was automatically detected on background-subtracted and binarized images using ImageJ analysis software (version 1.48, National Institutes of Health, Bethesda, MD, USA) to eliminate user bias. For neurogenesis analysis, the width of the granular cell layer (GCL) was measured using the measure tool in ImageJ. All image analyses were performed by a single individual with no knowledge of experimental group.

2.6. Neurobehavior assays

The open field assay was used to assess general locomotor function prior to learning and memory assays. Subjects were placed into a testing arena (48 cm × 48 cm × 48 cm), allowed 20 min of acclimation, and recorded for 10 min under lighting conditions of ~ 30 lx. A 3x3 grid of equal-sized squares was superimposed over the videos to create nine different movement zones. Locomotor activity was quantified using the number of times an individual crossed a grid line over the 10 min period. The total number of crossings were quantified and compared across experimental groups.

Learning and memory were assessed using the novel object recognition task performed as previously described (Berg et al., 2020). Briefly, subjects were habituated to an empty testing arena (48 cm × 48 cm × 48 cm) for 30 min prior to testing under lighting conditions of ~ 45 lx. The following day, subjects were again habituated to the arena followed by an introduction to two identical objects. Subjects were allowed 10 min to interact with these objects followed by an isolation period of 60 min. During the isolation period, the arena and objects were cleaned with 70% ethanol and one object was replaced with a novel object. At the end of the isolation period, subjects were returned to the arena and allowed 5 min to interact with the familiar and novel objects. The objects used were orange plastic cones and glass bell jars. The location and selection of novel objects within each trial was randomized. All phases were video recorded and the time spent sniffing each object was measured by experimenters blinded to experimental group. Data were transformed to calculate % preference for the novel object and an object discrimination index in order to correct for potential differences in exploration time between individuals (Gulinello et al., 2019).

Contextual and cued fear conditioning, performed as previously described (Berg et al., 2020), were used as a second assay of learning and memory. Briefly, subjects were trained to associate a specific context and cue with a foot shock (0.7 mA). The chambers (25 cm h × 32 cm w × 25 cm d) were brightly lit (~100 lx) with floors made of stainless-steel rods placed 1.6 cm apart (MedAssociates Inc., St. Albans, VT, USA). Test chambers were placed into a noise reducing chamber and a front-facing camera was used to record each session. On the first day (training day), subjects were trained in a context that included wire flooring, aluminum walls, and a vanilla scent (1:100 dilution of McCormick Vanilla Extract). The cue was an auditory cue of 80 dB white noise for 30 s. On the second test day (24 h post-training), subjects were placed back into the chambers for 5 min with the identical context but no audio cue or foot shock and the amount of time subject froze was measured. On the third test day (48 h post-training), subjects were placed in chambers in which the context had been altered to a smooth plastic floor, angled black walls, and a lemon scent (1:100 dilution of McCormick Lemon Extract). Subjects were monitored in this environment for 3 min before and 3 min after the auditory cue. The average motion index, a comprehensive measure of overall movement (Anagnostaras et al., 2000), was automatically quantified by VideoFreeze software (version 2.7; MedAssociates Inc.) to assess the movement of each subject during both the context and cue testing periods.

2.7. Statistical analyses

Two different models were considered for the dose-response data: 1) 2-parameter log-logistic model; and 2) probit model. For each, we considered a model in which the slope was allowed to differ at LD_{50}

for males and females (different shapes) as well as a model in which the slope of the dose response curve at the LD_{50} was constrained to be the same for males and females. Akaike Information Criterion was used to pick the model that best fit the data. Estimates of the LD_{20} and LD_{50} with 95% confidence intervals were determined for each sex using the delta method. The estimated LD_{20} and LD_{50} were compared between the sexes. These analyses were conducted using the *drc* package in R (Ritz and Streibig, 2005).

Key outcomes for the histology data included FJC (number of FJC-labeled cells/mm^2), GFAP (% area of immunoreactivity), S100β (% area of immunoreactivity), and IBA-1 (% area of immunoreactivity). Mixed-effects models, including animal-specific random effects, were fit to assess differences between exposure groups. Primary factors of interest included exposure (DFP, VEH), brain region (thalamus, piriform cortex, amygdala, hippocampus, cortex), sex (male, female), and time post-exposure (1, 7, 28 d). Interactions between the factors (exposure, brain region, sex, and time point) were considered and the best model was chosen using Akaike Information Criterion. Outcomes were transformed using the natural logarithm after shifting all values by 1 to enable the calculation for samples with no positive staining to better meet the assumptions of the model. Contrasts for exposure group and sex differences were constructed and tested using a Wald test. The Benjamini-Hochberg false discovery rate (FDR) was used within an outcome measure to account for multiple comparisons. Results are presented as geometric mean ratios (GMR) between exposure groups for the log-transformed outcomes. Point estimates of the ratios and 95% confidence intervals are presented in the figures. When the confidence interval for the GMR includes 1, there is no statistical evidence of a difference between groups. These analyses were performed using SAS software, version 9.4 and alpha was set at 0.05; all reported results remained significant after the FDR procedure.

Key outcomes for neurobehavior included open field (# grid crossings), novel object familiarization (sniff time), novel object test (% novel preference and discrimination index), and fear conditioning (average motion index). Neurogenesis outcomes included (% Ki67 immunopositive cells of total cells determined by DAPI staining), DCX (% area of immunoreactivity), NeuN (% area of immunoreactivity), and GCL width (μm). These outcomes were analyzed at 28 d and included only one brain region. Open field data were analyzed using a Mann-Whitney *U* test, while all other neurobehavior and neurogenesis outcomes were analyzed using a two-way ANOVA with *post-hoc* Holm-Sidak test where applicable. Each of these outcomes are presented as mean ± SEM with individual data points representing individual animals. These analyses were conducted in GraphPad Prism, version 8.2.1 with alpha set at 0.05.

3. Results

3.1. Acute effects of acute DFP intoxication in juvenile rats

Male and female rats were injected with varying doses of DFP at PND 28 and the percent animals surviving at 4 h post-injection was determined (Fig. 1**C**). The dose–response curve for DFP-induced mortality for females was shifted to the left of that for males (Fig. 1**D**). Of the statistical models used to fit the data, the best model considered was the 2-parameter log-logistic model with a common slope. The estimated LD_{20} and LD_{50} for males were 4.1 and 6.2 mg/kg, respectively. For females, the estimated LD_{20} and LD_{50} values were 2.9 and 4.4 mg/kg, respectively (Fig. 1**E**). While there was no statistical difference between these parameters, there was a trend towards increased susceptibility to acute DFP-induced lethality in females ($p = .08$). The ratio of effect doses at LD_{20} and LD_{50} for females to males was 0.70 (95% CI: 0.36, 1.03) indicating the dose is 30% lower in females than males at LD_{20} and LD_{50}. However, due to the lack of statistically significant differences between the LD_{20} and LD_{50} values for each sex, DFP was used at a dose of 3.4 mg/kg in both sexes for the remainder of the study.

Seizure behavior was monitored for 4 h following acute DFP intoxication using a seizure severity scale (Fig. 2**A**) adapted from an adult rat DFP model (Deshpande et al., 2010). Seizure scores were plotted over time (Fig. 2**B**), and the average seizure score over the 4 h period was calculated for each animal (Fig. 2**C**). Seizure behavior data were also quantified as the total duration of convulsive seizures (scores of ≥ 3; Fig. 2**D**). The average seizure scores and convulsive seizure duration were significantly higher in males than females ($p < .05$) (Fig. 2**C, 2D**). A seizure score of 3 or higher has been demonstrated to correspond with SE in the adult DFP rat (Deshpande et al., 2010; Phelan et al., 2015). The majority of DFP males (86.6%) exhibited a seizure score ≥ 3 at least once during the 4 h post-exposure; whereas, only 53.3% of DFP females reached a score of 3 during the 4 h seizure monitoring period (Fig. 2**E**).

To confirm that differences in seizure behavior were not due to sex differences in DFP disposition in the brain of male versus female juvenile rats, AChE, BChE, and total ChE activity were measured in cortical brain samples at 1 d post-DFP. Baseline cholinesterase levels in VEH animals were comparable between sexes, and AChE was inhibited to the same extent in males and females following DFP exposure (Fig. 2**F**). The majority of cholinesterase inhibition in both sexes was driven by inhibition of AChE, as minimal BChE activity was detected in either sex in the absence or presence of DFP.

EEG recordings obtained from a different cohort of animals were used to confirm epileptiform activity in both sexes. EEG traces illustrate increased brain activity in juvenile males and females following DFP intoxication, as measured by increased amplitude and frequency of the spike events (Fig. 3**A**). Quantitative analyses of EEG recordings from males and females for 2 h post-DFP support the onset of sustained seizure activity following DFP intoxication and are consistent with the behavioral seizure data in demonstrating a greater seizure response in males compared to females (Fig. 3**B**).

3.2. Sex-specific neuropathologic effects of acute DFP intoxication in juvenile rats

Neurodegeneration is a well-documented consequence of acute OP intoxication in adults (reviewed in Chen, 2012). Using FJC staining to visualize degenerating neurons (Schmued et al., 2005) (Fig. 4**A**), we observed significantly increased FJC staining in DFP animals that varied by time post-exposure ($p < .001$), sex ($p < .001$) and by brain region ($p < .001$) (Fig. 4**B**). In both males and females, DFP-exposed animals had higher FJC staining than VEH animals across days and regions (GMR > 2.0, $p < .042$) with the exception of the female somatosensory cortex at 1 d post-exposure ($p = .19$). The difference between DFP and VEH animals tended to be higher in males than in females, which was driven by higher FJC staining in male DFP animals compared to female DFP animals (GMR = 3.4, 95% CI = 2.0–5.8, $p < .001$).

Antibodies specific to GFAP and S100β are reported to label unique astrocyte populations in the brain, especially during neurodevelopment (reviewed in Holst et al., 2019). GFAP immunoreactivity (Fig. 5**A**) revealed sex-specific changes in expression following DFP intoxication. The difference in percent positive GFAP staining area between DFP and VEH animals varied by sex ($p = .02$) and both time and region ($p < .001$) (Fig. 5**B**). Differences in GFAP between DFP and VEH animals were limited at 1 d post-exposure, with the only significant difference observed in the male hippocampus (GMR = 1.4, 95% CI = 1.1–1.9, $p = .007$). By 7 d post-exposure, GFAP levels were significantly elevated in DFP animals compared to VEH animals in all brain regions and both sexes ($p < .02$) with the exception of the female somatosensory cortex (GMR = 1.3, 95% CI = 0.9–1.8, $p = .1$). Elevated GFAP levels in DFP compared to VEH animals

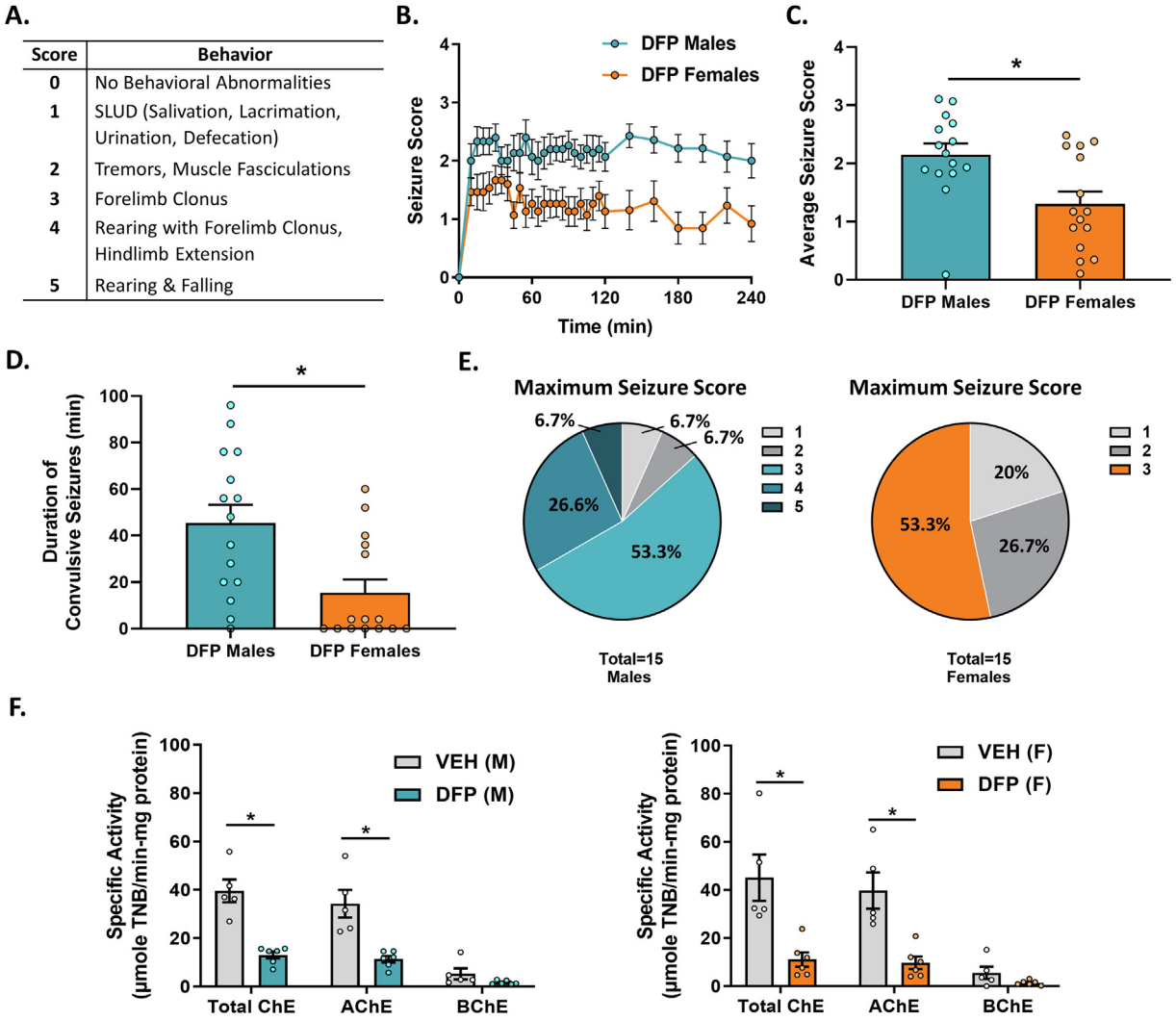

Fig. 2. Juvenile males exhibit more severe seizure behavior than age-matched females following DFP. (**A**) Seizure behavior scale used to score seizure behavior of juvenile male and female rats following acute intoxication with DFP at 3.4 mg/kg, s.c. (**B**) Temporal profile of seizure scores from males and females during the first 4 h post-DFP exposure. (**C**) Average seizure score and (**D**) average duration of convulsive seizures in DFP-intoxicated males and females. Data presented as mean ± SEM with individual data points per animal (n = 15/group); *p < .05 as determined by Mann Whitney test. (**E**) Maximum seizure score reached at any point during the 4 h monitoring period in DFP-intoxicated males (left) and females (right). (**F**) The enzymatic activity of acetylcholinesterase (AChE) in cortical tissue from males (left) and females (right) at 1 d post-exposure to VEH or DFP. Data presented as mean ± SEM with individual data points per animal (n = 5–6 per group); *p < .05 as determined by two-way ANOVA with *post hoc* Holm-Sidak test.

persisted in males at 28 d post-exposure in all brain regions except the somatosensory cortex (GMR = 1.4, 95% CI = 1.0–2.0, p = .06). In contrast, in females, the only significant difference between DFP and VEH at 28 d post-exposure was in the amygdala (GMR = 1.3, 95% CI = 1.1–1.5, p = .01).

The difference in S100β immunoreactivity (Fig. 6**A**) between DFP and VEH animals varied by time (p = .04) and sex (p = .005) with a trend for a difference by region (p = .1) (Fig. 6**B**). At 1 d post-exposure, male DFP animals had increased S100β relative to male VEH animals in the piriform cortex (GMR = 1.4, 95% CI = 1.1–1.7, p = .002) and the thalamus (GMR = 1.5, 95% CI = 1.1–1.9, p = .003). There were no significant differences between DFP and VEH females at 1 d post-exposure (p > .3). S100β levels were significantly increased in both male and female DFP animals on d 7 post-exposure in the amygdala (male: GMR = 1.8, 95% CI = 1.5–2.2, p < .001; female: GMR = 1.4, 95% CI = 1.1–1.7, p = .004), piriform cortex (male: GMR = 1.9, 95% CI = 1.6–2.3, p < .001; female: GMR = 1.5, 95% CI = 1.2–1.8, p < .001) and thalamus (male: GMR = 2.0, 95% CI = 1.6–2.5, p < .001; female: GMR = 1.5, 95% CI = 1.2–1.8, p < .001). At 7 d post-exposure, DFP males had elevated S100β expression compared to VEH males in the hippocampus (GMR = 1.6, 95% CI = 1.3–2.0, p < .001) and cortex (GMR = 1.7, 95% CI = 1.3–2.1, p < .001). By d 28 post-exposure, S100β remained elevated in all brain regions for males, but just in the piriform cortex and thalamus for the females. Within the DFP group, there was no significant difference in S100β immunoreactivity between males and females (GMR = 1.1, 95% CI = 0.9–1.2, p = .4).

IBA-1 and CD68 immunoreactivity were used to quantify microglia and phagocytosis, respectively, in the brain (Fig. 7**A**). CD68 was not present at measurable levels in any group and was, therefore, excluded from data analysis. The difference between DFP and VEH animals in percent area of IBA-1 immunostaining varied only by d post-exposure (p = .005), and data were, therefore, pooled across sexes (Fig. 7**B**). There was no significant difference between groups 1 d post-exposure (GMR = 1.1, 95% CI = 0.9–1.3, p = .4), but there was significantly higher IBA-1 in DFP animals compared to VEH on d7 (GMR = 1.7, 95% CI = 1.4–2.1, p < .001) and 28 (GMR = 1.6, 95% CI = 1.3–2.0, p < .001) post-exposure.

A.

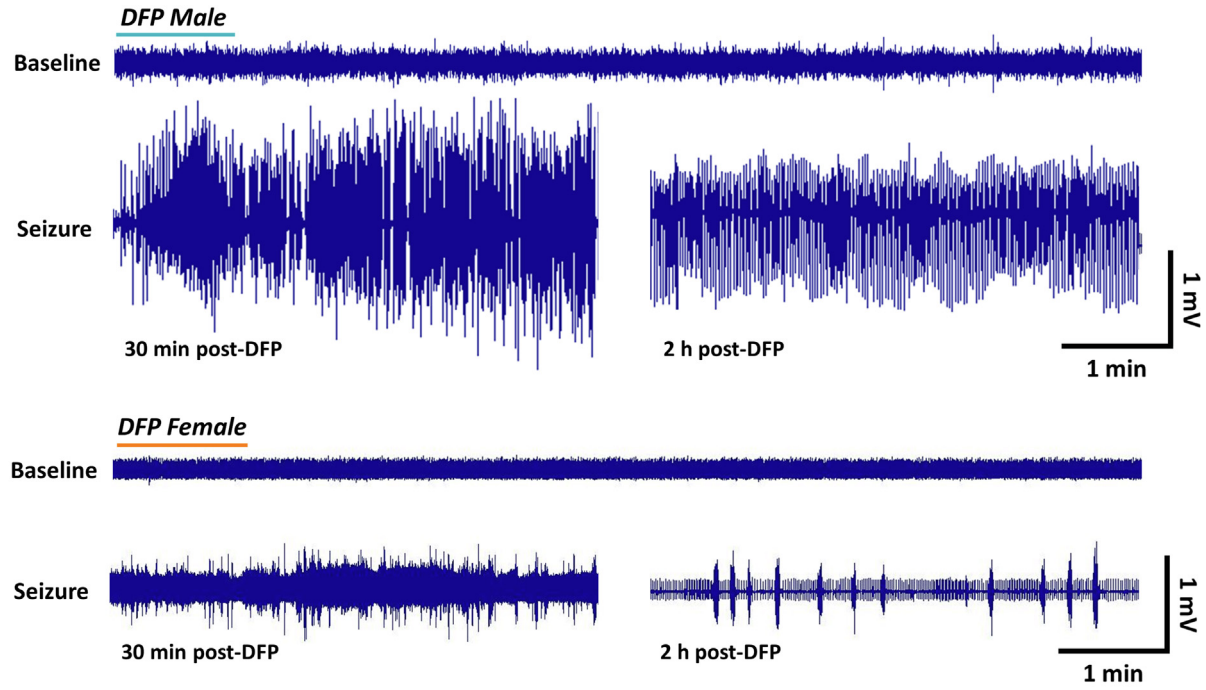

B.

	Spike Amplitude (Root Mean Squared, μV)		Spike Frequency (# spikes/s above baseline)	
	Baseline	Seizure	Baseline	Seizure
Male 1	24.50	113.47	3.37	21.29
Male 2	18.04	48.06	0.73	9.10
Male 3	20.19	74.32	1.54	16.71
Female 1	18.42	40.04	1.47	9.85
Female 2	21.47	21.69	2.39	2.41

Fig. 3. Electroencephalographic (EEG) seizure activity appears greater in males than females following acute DFP intoxication. (**A**) Representative EEG traces during the baseline (pre-DFP) and seizure (post-DFP) periods in a male and female animal. (**B**) Quantitative EEG data showing spike amplitude and frequency in 3 males and 2 females during the baseline and the first 2 h post-DFP.

3.3. Neurobehavioral effects of acute DFP intoxication

The open field assay was used to quantify motor abilities prior to the start of learning and memory testing. Locomotor activity was comparable between VEH and DFP groups in both male ($p = .29$) and female ($p = .33$) animals (Fig. 8**A**). Novel object recognition was used to test memory function following object familiarization. The familiarization period indicated no preexisting side preference/salience or avoidance in VEH males ($p = .89$), DFP males ($p = .7$), VEH females ($p = .8$), or DFP females ($p = .49$) (Fig. 8**B**), as previously shown for these objects in rats (Berg et al., 2020). Performance during the test period was analyzed using % novel preference and a discrimination index, two transformations of raw data that account for investigation time (Gulinello et al., 2019). DFP males showed significant deficits by both % novel preference ($p < .001$) and discrimination index ($p < .001$) relative to their VEH controls (Fig. 8**C**). Similarly, DFP females also showed significant deficits relative to VEH females as determined using both the % novel preference ($p = .02$) and discrimination index ($p = .02$) metrics (Fig. 8**C**). While both sexes showed statistically significant deficits, the magnitude of change between VEH and DFP animals was greater in males than females with respect to novel object preference and discrimination index.

Performance in contextual and cued fear conditioning was used to corroborate learning and memory deficits identified in the novel object recognition task. Freezing behavior in response to a fearful stimulus was quantified using the average motion index, a comprehensive measure of animal movement. No significant differences in movement were detected during the baseline period (pre-training) between the VEH and DFP groups of each sex. During the test periods, DFP males showed significantly increased motion compared to VEH males during both the context ($p = .002$) and cue ($p = .005$) tests (Fig. 9**A**). DFP females showed significantly increased motion compared to VEH females in the context ($p = .005$) but not cue ($p = .11$) test (Fig. 9**B**).

3.4. Acute DFP intoxication alters neurogenesis in a sex-specific manner

A period of extensive neurogenesis occurs in the rodent brain during the early perinatal period; however, it continues at a reduced rate in the subgranular zone (SGZ) of postnatal and adult animals (Kempermann et al., 2015; Toda and Gage, 2018). Changes in hip-

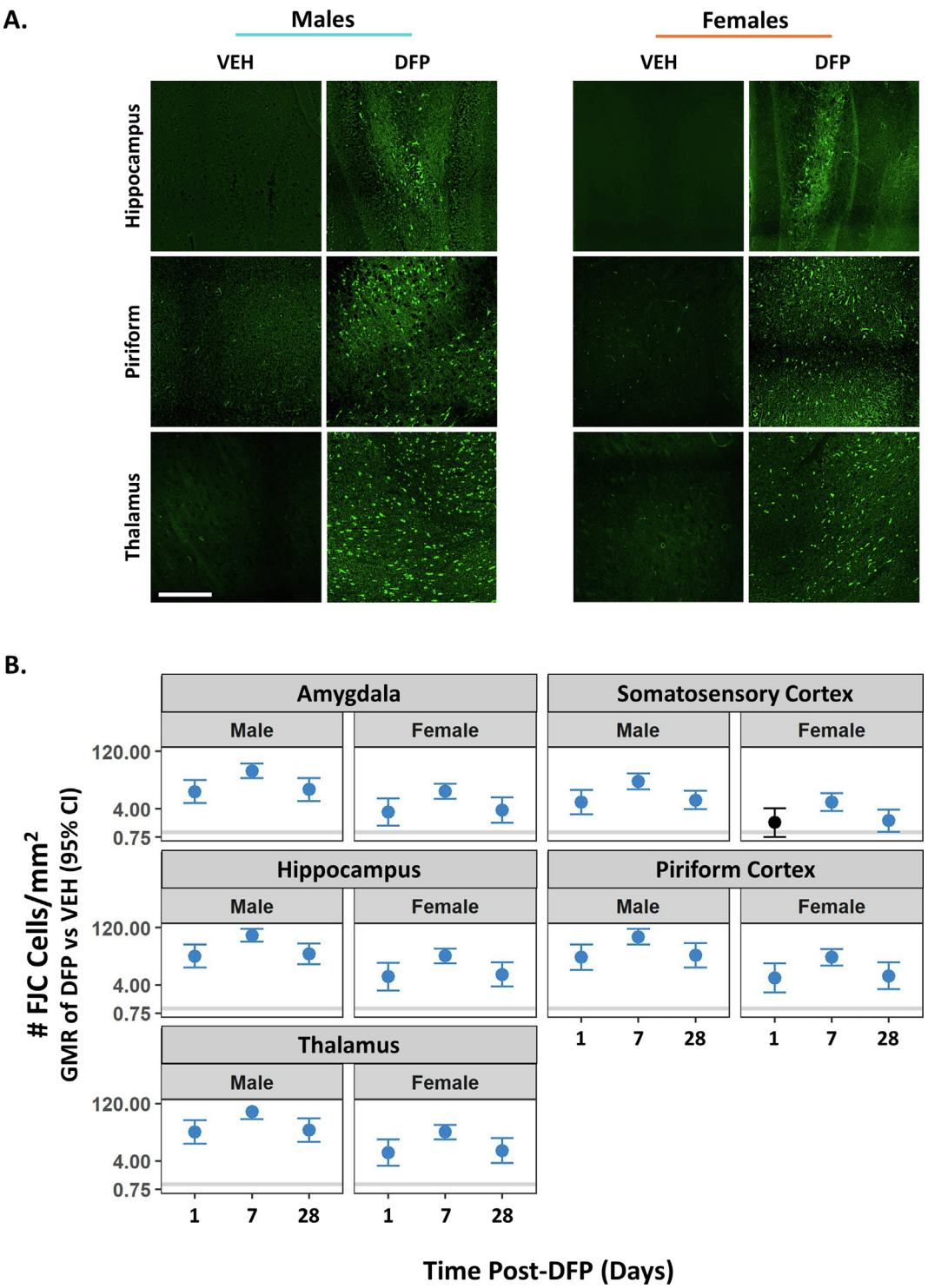

Fig. 4. DFP causes significant neurodegeneration in both male and female rats. (**A**) Representative photomicrographs of Fluoro-Jade C (FJC) staining in the hippocampus, piriform cortex, and thalamus of VEH and DFP intoxicated rats at 7 d post-intoxication. Bar = 100 μm. (**B**) The number of FJC-labeled cells was quantified in multiple brain regions of each sex at 1, 7, and 28 d post-DFP injection. Hippocampus includes dentate gyrus, CA1, and CA3 subregions. Data shown as the geometric mean ratio of DFP vs. VEH with 95% confidence intervals. Confidence intervals entirely above or below 1 are colored blue and indicate a significant difference between the two groups being compared at $p < .05$ (n = 5–7 animals/group). (For interpretation of the references to colour in this figure legend, the reader is referred to the web version of this article.)

pocampal neurogenesis following acute DFP intoxication were evaluated by quantifying biomarkers of immature neurons (DCX immunoreactivity) and proliferating cells (Ki67 immunoreactivity) in the SGZ (Kee et al., 2002; Couillard-Despres et al., 2005). Structural changes in the dentate gyrus of the hippocampus were evaluated by quantifying NeuN immunoreactivity, a biomarker of mature neurons, and the width of the granule cell layer (GCL) (Fig. 10**A**). DFP males showed a significant increase in the number of $Ki67^+$ cells in the SGZ compared to their VEH counterparts ($p < .001$), while there was no difference between female DFP and VEH animals ($p = .8$; Fig. 10**B**). A

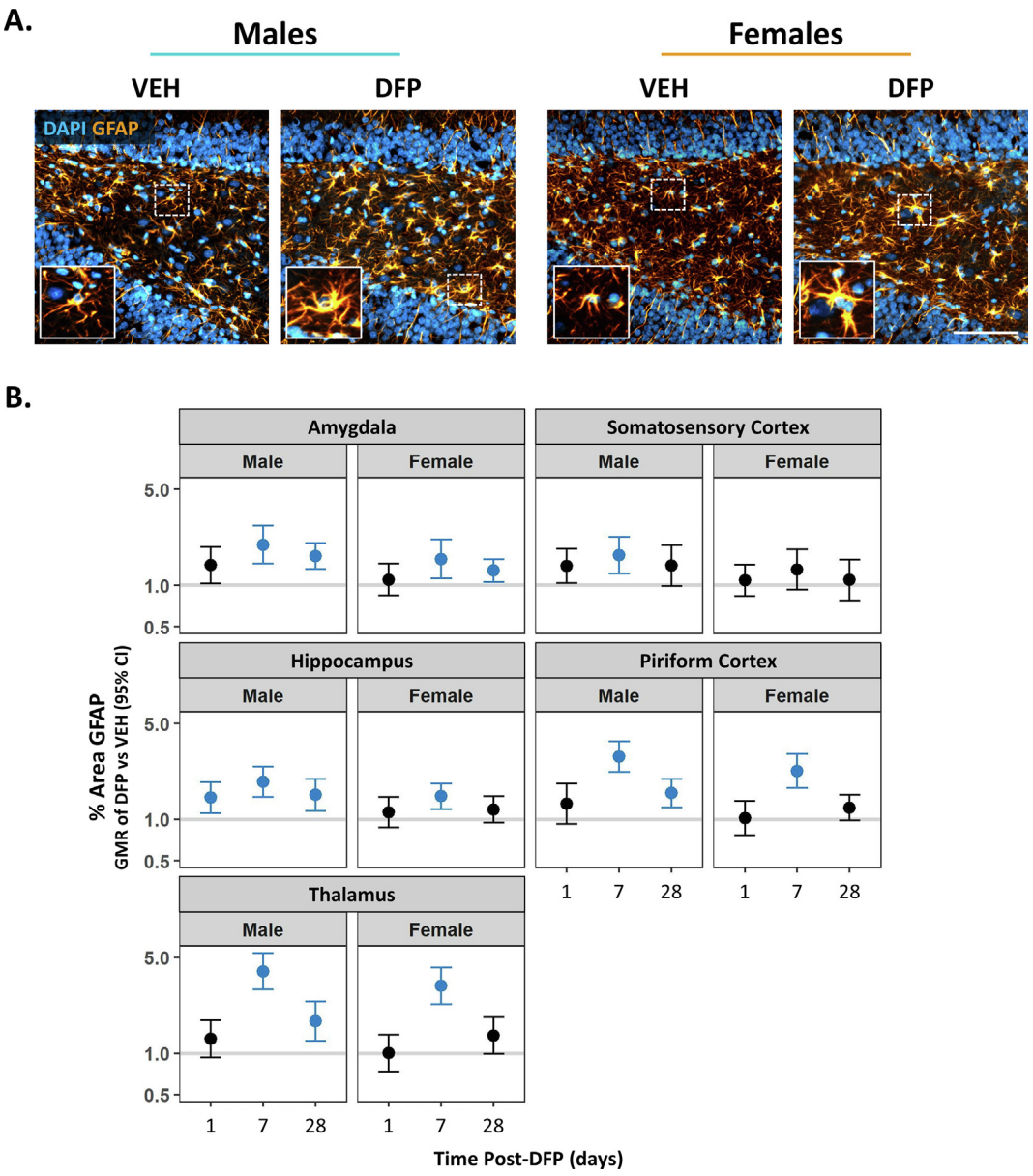

Fig. 5. DFP increases GFAP immunoreactivity in a time, region, and sex-dependent manner. (**A**) Representative photomicrographs of GFAP immunostaining (astrocytes and radial glia; orange) in the hippocampus of VEH and DFP rats at 7 d post-intoxication. Blue = DAPI (cell nuclei). Bar = 100 μm. (**B**) The % area of GFAP immunoreactivity was quantified in multiple brain regions of each sex at 1, 7, and 28 d post-DFP injection. Hippocampus includes dentate gyrus, CA1, and CA3 subregions. Data shown as the geometric mean ratio of DFP vs. VEH with 95% confidence intervals. Confidence intervals entirely above or below 1 are colored blue and indicate a significant difference between the two groups being compared at $p < .05$ (n = 5–7 animals/group). (For interpretation of the references to colour in this figure legend, the reader is referred to the web version of this article.)

similar trend was observed in DCX immunoreactivity, where DFP males had significantly higher levels than VEH males ($p = .005$; Fig. 10**C**), but no differences in DCX immunoreactivity were observed between DFP and VEH females ($p = .074$; Fig. 10**C**). There were no effects of DFP on NeuN immunoreactivity in either male ($p = .83$) or female animals ($p = .13$) subjects compared to their VEH counterparts (Fig. 10**D**). Similarly, DFP did not cause any changes in GCL width in either males ($p = .94$) or females ($p = .4$) compared to their respective VEH groups (Fig. 10**E**).

4. Discussion

The majority of published studies on the neurotoxicity of acute intoxication with OP threat agents are focused on the adult male brain. Here, we characterized the acute and chronic neurotoxic effects in male and female rats acutely intoxicated with DFP at PND 28. With respect to brain development and sexual maturation, rats at PND 28 – PND 56, the age range over which we examined neurotoxic outcomes in this study, correspond to 4–11 year old humans (Semple et al., 2013; Zhang et al., 2019). Our quantification of acute seizure activity and mortality, as well as chronic neurological damage, in juvenile male and female rats identified sex-specific neurotoxic effects of DFP. Overall, juvenile males showed more severe behavioral seizure and brain epileptiform activity immediately following acute DFP intoxication compared to juvenile females, despite having comparable AChE levels. Both juvenile male and female rats presented with significant neuropathology following DFP intoxication, although males had greater brain damage with respect to the extent (number of brain regions involved) and persistence of neurodegeneration and astroglio-

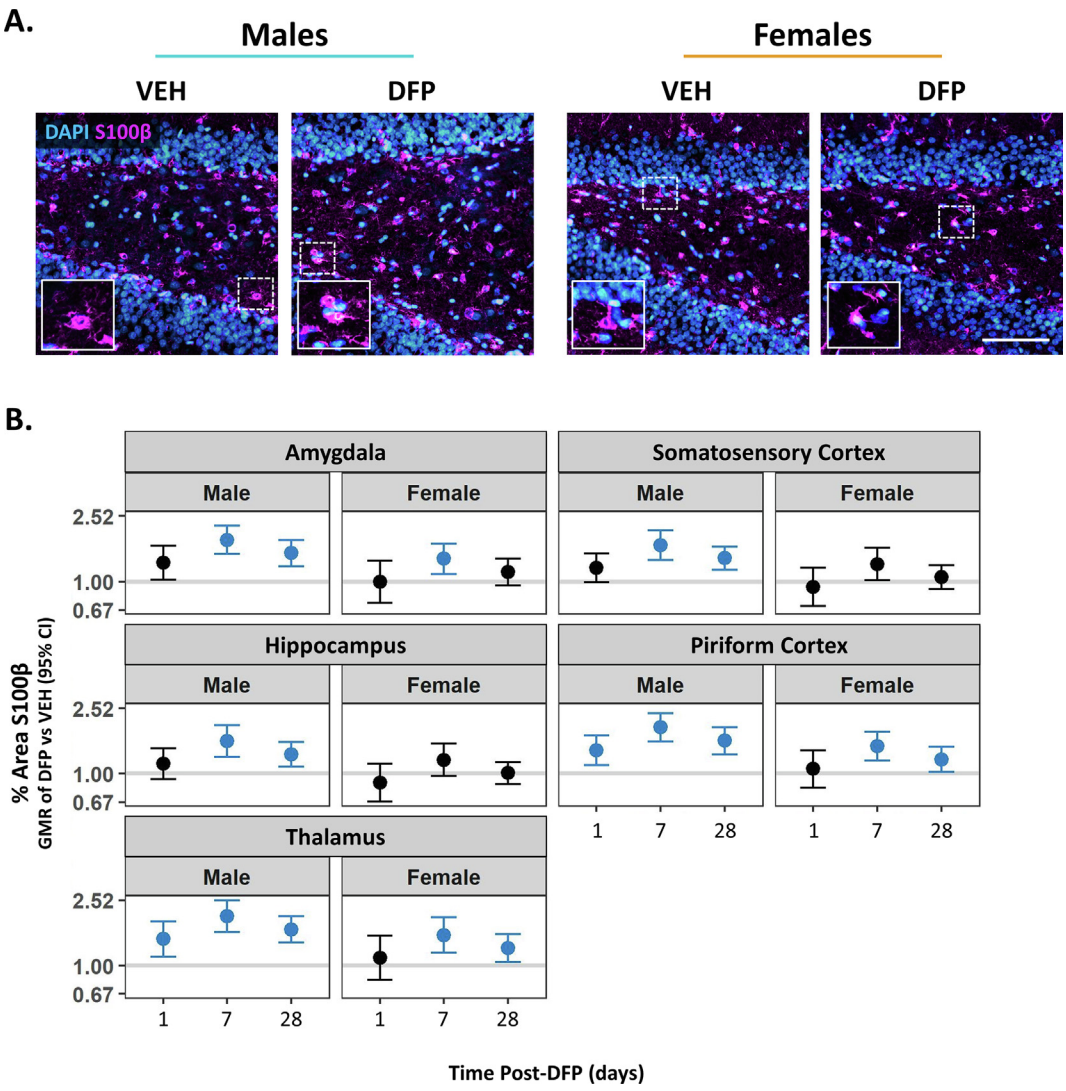

Fig. 6. DFP increases S100β immunoreactivity in a time, region, and sex-specific manner. (**A**) Representative photomicrographs of S100β immunostaining (mature astrocytes; magenta) in the hippocampus of VEH and DFP rats at 7 d post-intoxication. Blue = DAPI (cell nuclei). Bar = 100 μm. (**B**) The % area of S100β immunoreactivity was quantified in multiple brain regions of each sex at 1, 7, and 28 d post-DFP injection. Hippocampus includes dentate gyrus, CA1, and CA3 subregions. Data shown as the geometric mean ratio of DFP to VEH with 95% confidence intervals. Confidence intervals entirely above or below 1 are colored blue and indicate a significant difference between the two groups being compared at $p < .05$ (n = 5–7 animals/group). (For interpretation of the references to colour in this figure legend, the reader is referred to the web version of this article.)

sis. In contrast, microglial activation, which was found to be the most persistent outcome, did not differ by sex. Both males and females exhibited cognitive deficits but only males had significant changes in neurogenesis.

An initial dose-range finding study revealed comparable mortality curves between male and female animals. The similarities between curves are unsurprising in light of the steep dose–response relationship of OP lethality that is well-documented in OP threat agent models (Fawcett et al., 2009). Regarding seizure activity, DFP elicited significantly higher seizure behavior scores in males, with ~ 25% of males exhibiting clear generalized seizures. In contrast, the most severe seizure observed in females was forelimb clonus. EEG recordings from a separate cohort of animals confirmed DFP-induced neurological hyperactivity and increased spiking events in each sex and supported the observations of more severe behavioral seizures in males relative to females. Notably, the behavioral seizure response observed in our juvenile rat DFP model is less severe than has been previously reported for adult rat DFP models using nearly identical seizure scales (Gage et al., 2020; Supasai et al., 2020), suggesting age-specific seizure responses to DFP. This interpretation is supported by a recent publication that found seizure susceptibility to DFP increased significantly with age, ranging from the early postnatal period into young adulthood (Scholl et al., 2018). This is consistent with literature demonstrating increased expression of cholinergic and glutamatergic receptors between the post-weaning period (~PND 28) and early adulthood (~PND 60) in rats (Akazawa et al., 1994; Monyer et al., 1994; Jett, 1998). Although EEG activity was only recorded from a small cohort of animals that were not scored for seizure behavior, it has been demonstrated that seizure behavior is highly correlated with electrographic seizure activity in both male and female models of acute OP intoxication (Tanaka et al., 1996; McDonough and Shih, 1997; Gage et al., 2020).

The observed sex difference in seizure activity in juvenile rats after acute OP intoxication is consistent with other models of chemical-induced seizures. For example, adult female rats have been reported to have less severe SE than male rats in response to pilocarpine (Scharfman and MacLusky, 2014) or DFP (Gage et al., 2020). While the mechanistic underpinnings of this sex difference are unknown, a

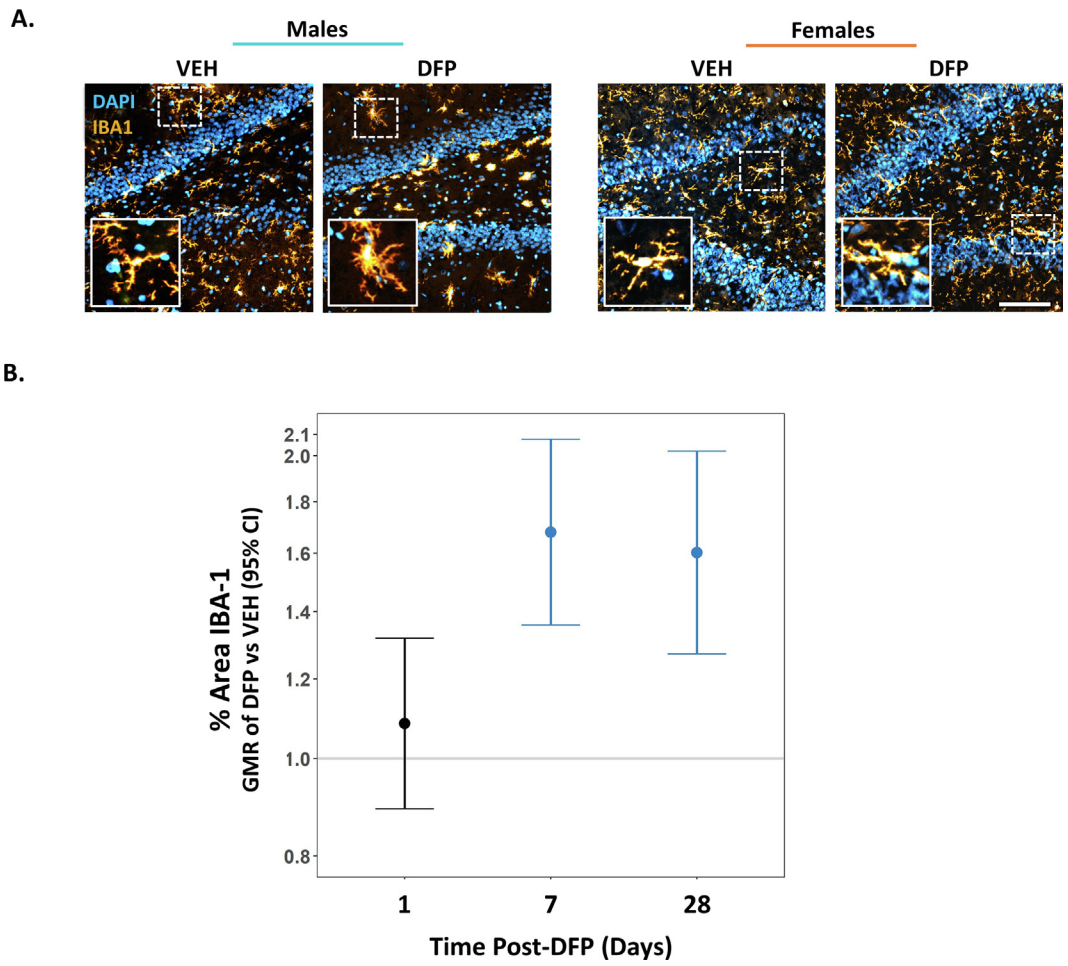

Fig. 7. DFP induces persistent microgliosis in both males and females. (**A**) Representative photomicrographs of IBA1 immunostaining (microglia; orange) in the hippocampus of VEH and DFP rats at 7 d post-intoxication. Blue = DAPI (cell nuclei). Bar = 100 μm. (**B**) The % area of IBA-1 immunoreactivity was quantified in multiple brain regions of each sex at 1, 7, and 28 d post-DFP injection. No effects of sex or brain region were observed, so data were collapsed across those variables. Data are shown as the geometric mean ratio of DFP to VEH with 95% confidence intervals. Confidence intervals entirely above or below 1 are colored blue and indicate a significant difference between the two groups being compared at $p < .05$ ($n = 5–7$ animals/group). (For interpretation of the references to colour in this figure legend, the reader is referred to the web version of this article.)

few hypotheses have been proposed. One hypothesis involves sex hormones (Velíšková and Desantis, 2013); however, it is unlikely that sex hormones are driving the differential seizure behavior we observed in this study because PND 28 rats have yet to experience a hormonal surge (Bell, 2018). Further, it was recently reported that estrous stage has no impact on seizure susceptibility in adult rats acutely intoxicated with DFP (Gage et al., 2020). Rather, it is more likely that the divergent seizure activity between males and females reflects the sexually dimorphic expression of excitatory and inhibitory receptors in the brain. Males and females have differential expression patterns of glutamatergic, cholinergic, and GABAergic receptors in the brain, each of which plays an important role in seizure induction and maintenance (Akman et al., 2014; Scharfman and MacLusky, 2014). Glutamate receptors, including NR1, NR2A, and GluR1, are critical for seizure maintenance following OP intoxication (Barker-Haliski and White, 2015; Hanada, 2020) and are reported to be expressed at higher levels in males than females during neurodevelopment (Hsu et al., 2000; Bian et al., 2012; Damborsky and Winzer-Serhan, 2012). Similarly, cholinergic receptor mRNA expression is higher in males than in females (Potier et al., 2005). Lastly, it is well-documented that females have greater expression of $GABA_A$ receptor mRNA and protein than males throughout postnatal brain development (Ravizza et al., 2003; Li et al., 2007; Chudomel et al., 2009). The greater expression of excitatory receptors and reduced expression of inhibitory receptors in males relative to females likely contributes to observed sex differences in seizure severity.

Despite the difference in acute seizure response, both DFP males and females showed significant neurodegeneration throughout the brain. This is consistent with recent evidence that acute DFP intoxication can induce brain damage independent of seizure activity in adult rats (González et al., 2020), and with the human literature indicating that acute intoxication with OPs can cause significant brain damage even at non- or subconvulsive doses (reviewed in Chen, 2012). It may also be the case that spontaneous recurrent seizures (SRS), which have been reported in adult male rats following acute DFP intoxication (Guignet et al., 2020; Putra et al., 2019), contributed to the sustained neurodegeneration observed in both sexes, but further research to confirm that acute OP intoxication causes SRS in juvenile rats is needed to address this hypothesis. Regarding regional damage, the thalamus, piriform cortex, and hippocampus were severely damaged in both male and female juveniles, which is similar to the regional patterns of brain damage reported in adult rats acutely intoxicated with DFP (Siso et al., 2017).

Neurodegeneration is often associated with neuroinflammation, which is a complex set of cellular and molecular processes triggered in response to insults within the nervous system (Guignet and Lein, 2018). The regional effects of DFP on neuroinflammation in the juvenile rat model mirrored the regional effects of DFP on neurodegenera-

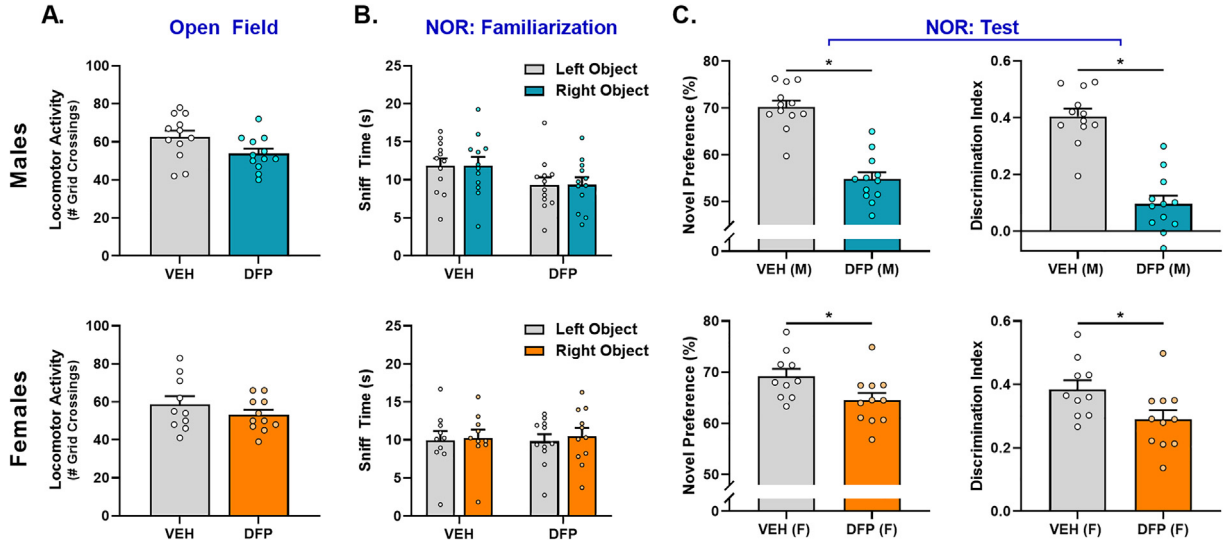

Fig. 8. Acute DFP intoxication impairs recognition memory in both males and females at 1 month post-exposure. (**A**) Open field data showing locomotor activity in male and female rats as measured by the number of grids crossed in an open arena (48 cm^3) with a 3x3 grid overlay. Novel object recognition data showing sniff time with each object during the familiarization (**B**) and test (**C**) phases of the assay. The familiarization phase compares left vs right objects to ensure there are no inherent biases in side preference. Data from the test phase were analyzed to represent both the novel preference (%) and the discrimination index between VEH and DFP rats of each sex. Data presented as mean ± SEM with individual data points per animal (n = 10–12/group); *p < .05 as determined by Mann-Whitney *U* test or two-way ANOVA. NOR = novel object recognition.

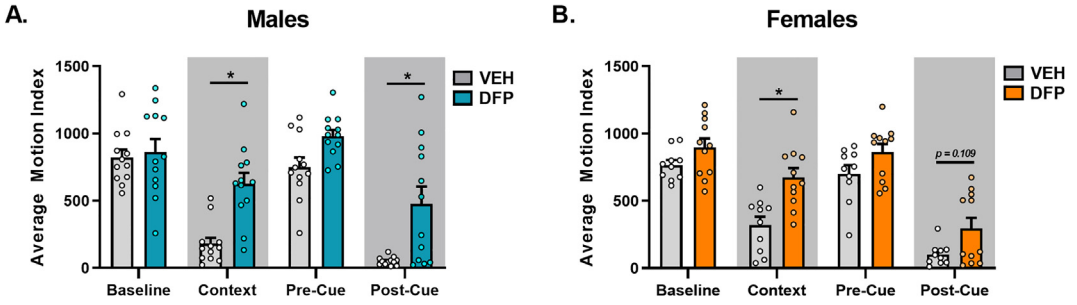

Fig. 9. DFP males show more pronounced fear-associated memory deficits than DFP females. Movement patterns of VEH and DFP male (**A**) and female (**B**) rats as measured by the average motion index during the baseline, context, and cue periods. Gray shading highlights test periods where subjects were expected to freeze or reduce motion. Data presented as mean ± SEM with individual data points per animal (n = 10–12/group); *p < .05 as determined by two-way ANOVA with *post hoc* Holm-Sidak test.

tion and were largely comparable to the adult DFP model (Siso et al., 2017), with some of the most severe inflammation occurring in the piriform cortex, thalamus, and hippocampus. Two primary neuroimmune cell types, microglia and astrocytes, are known to be activated in the adult brain for months following acute DFP intoxication (Gage et al., 2020; Supasai et al., 2020). This response typically coincides with increased levels of pro-inflammatory cytokines, sustained neuronal injury, and an aberrant phagocytic response that may further damage healthy cells (reviewed in Guignet and Lein, 2018). In our experimental juvenile model, DFP males exhibited significantly increased immunoreactivity for GFAP and S100β, both biomarkers of astrocytes, throughout the brain at 7 and 28 d post-exposure, with the highest levels of expression in the piriform cortex and thalamus. Juvenile females also showed astrogliosis following DFP, but it was less persistent compared to DFP males. This astrocytic response differs slightly from that of adults, which have shown a significant increase in GFAP immunoreactivity as early as 4 h post-DFP (Liu et al., 2012). The observed sex difference likely reflects sex differences in the severity of seizure activity, since it has previously been shown that seizure severity is predictive of the extent and persistence of neuroinflammation in adult models of acute DFP intoxication (Kuruba et al., 2018; Hobson et al., 2019). Interestingly, there was no effect of sex on microglial activation, which was increased throughout the brain at 7 and 28 d post-DFP. This is consistent with observations of the adult DFP model that microglial activation is more persistent than the astrocytic response (Supasai et al., 2020).

Acute DFP intoxication impaired cognitive function in both sexes. No differences were observed in locomotor function between DFP and VEH animals of either sex, eliminating a potentially confounding variable on learning and memory assays. DFP males exhibited slightly poorer cognitive performance than DFP females as reflected by significant deficits in both cue and context fear conditioning. Previous literature demonstrated that neuropathology, most notably neurodegeneration and microglial activation, temporally coincided with behavioral deficits following acute DFP intoxication in adult rats (Flannery et al., 2016; Guignet et al., 2020). Similarly, other models of acute OP intoxication have reported positive correlations between initial neuropathology and subsequent cognitive impairment (de Araujo Furtado et al., 2012; Reddy et al., 2020). Neuroinflammation has been proposed to be a contributing factor to cognitive dysfunction following chemical-induced seizures (Guignet and Lein, 2018). While sex differences in reactive astrogliosis and neurogenesis were observed in our

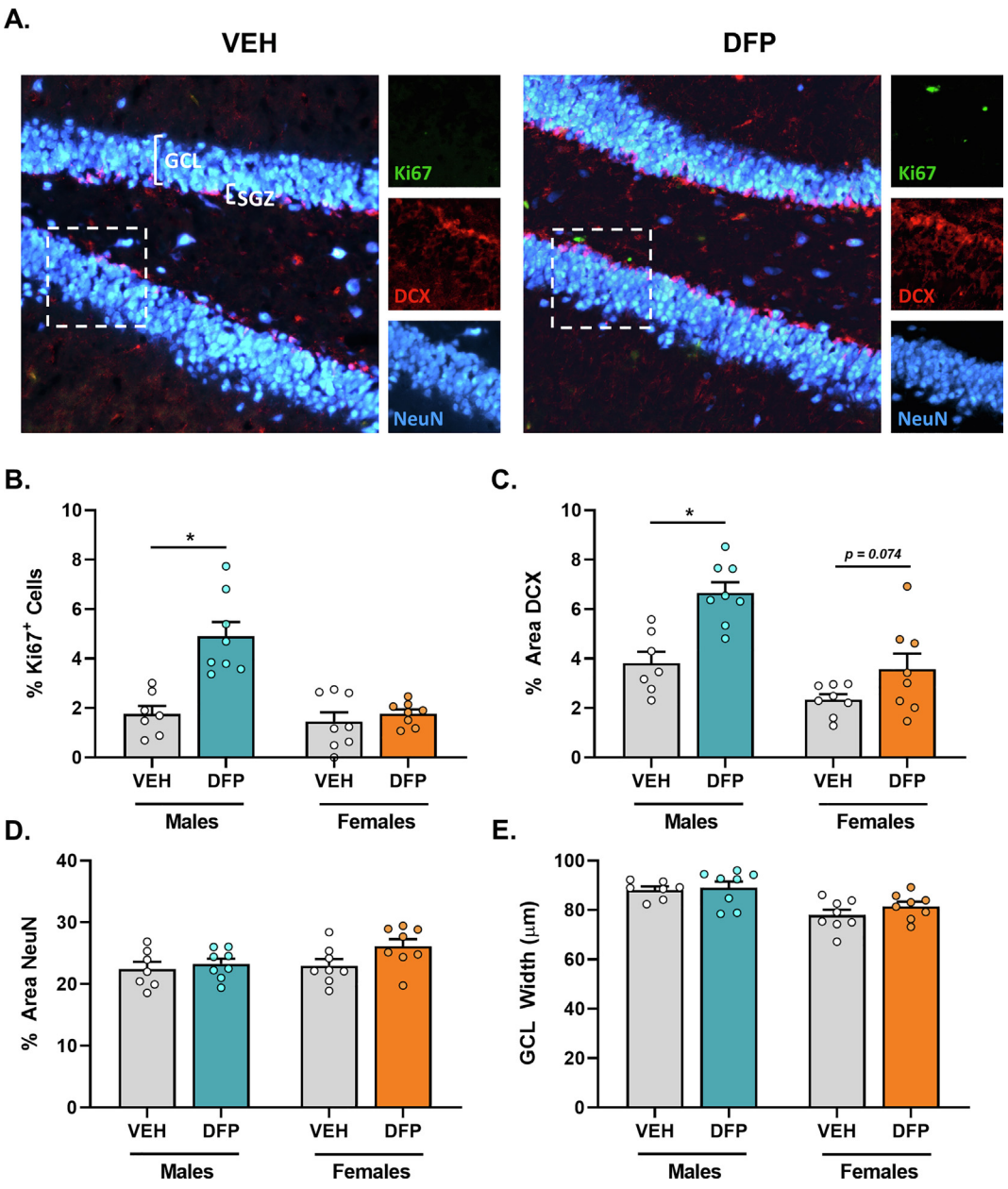

Fig. 10. DFP increases neurogenesis markers in males but does not elicit obvious **structural changes in the hippocampus at 28 d post-intoxication.** (**A**) Representative photomicrographs of Ki67 (proliferating cells), doublecortin (DCX; immature neurons), and NeuN (mature neurons) in the hippocampus of VEH vs DFP male rats. No differences between VEH and DFP were observed in female rats. Proliferating cells were quantified using the % Ki67$^+$ cells (**B**) and the % area of DCX$^+$ staining (**C**). Mature neurons were quantified using the % area of NeuN$^+$ staining (**D**) and the width of the hippocampal granule cell layer (GCL; **E**). Data presented as mean ± SEM with individual data points per animal (n = 6–8/group); *p < .05 as determined by two-way ANOVA with *post hoc* Holm-Sidak test.

model, both sexes experienced comparable microglial activation and cognitive deficits, both of which were present at 1 month post-DFP. This congruence between sexes suggests microglial-mediated neuroinflammation plays a more predominant role in learning and memory impairments following acute OP intoxication.

Hippocampal neurogenesis is critical to cognitive function (Lazarov and Hollands, 2016) and increased neurogenesis is well-documented following pilocarpine-induced SE (Varodayan et al., 2009; Wu et al., 2019; Velazco-Cercas et al., 2020). Our results revealed that DFP males, who experienced prolonged convulsive seizures, exhibited increased hippocampal neurogenesis, but DFP females did not exhibit any significant change in neurogenesis. If females indeed have less severe SE than males, the lack of neurogenic effects in DFP females support the previously reported positive relationship between convulsive seizure duration and neurogenesis following chemical-induced SE (Yang et al., 2008; Hung et al., 2012). It has also been reported that males are more susceptible to changes in hippocampal signaling and plasticity than females during development (Zitman and Richter-Levin, 2013). The increased neurogenesis observed in males may also contribute to the slightly more severe cognitive deficits that males displayed compared to females, as aberrant hippocampal neurogenesis has been shown to directly contribute to cognitive decline following acute OP-induced seizures (Cho et al., 2015). However, given the presence of cognitive deficits in DFP females independent of changes in neurogenesis, it appears more likely that the neurogenic response is determined by seizure severity and has minimal relationship to cognitive deficits associated with acute DFP intoxication.

To conclude, the present study describes a juvenile rat model of OP-induced SE that identified sex differences in both acute and chronic responses to acute DFP intoxication. Our findings motivate future studies to characterize whether the sex-specific effects of acute DFP intoxication primarily reflect biological sex, initial seizure severity, or some combination of the two. These data also point to microglial-mediated neuroinflammation as a likely mechanism contributing to long-term cognitive deficits following acute OP intoxication in juvenile animals. The temporal relationship between microglial activation and neurobehavioral deficits in both sexes, despite the sex differences observed in other endpoints, highlights the potential for microglia to play a critical role in the long-term neurological consequences of acute OP intoxication. Taken together, these data represent an important step in the development of experimental models to test candidate medical countermeasures for treatment of children in the event of a chemical emergency involving OPs. Our findings also reinforce the need to provide medical attention and follow-up to all exposed individuals, regardless of acute seizure response.

CRediT authorship contribution statement

Eduardo A. González: Conceptualization, Methodology, Data curation, Investigation, Writing - original draft, Visualization. **Jonas J. Calsbeek:** Methodology, Investigation, Writing - review & editing. **Yi-Hua Tsai:** Methodology, Investigation, Writing - review & editing. **Mei-Yun Tang:** Methodology, Investigation, Writing - review & editing. **Peter Andrew:** Investigation, Writing - review & editing. **Joan Vu:** Investigation, Writing - review & editing. **Elizabeth L. Berg:** Investigation, Writing - review & editing. **Naomi H. Saito:** Formal analysis, Writing - original draft, Writing - review & editing, Visualization. **Danielle J. Harvey:** Formal analysis, Writing - original draft, Writing - review & editing, Visualization. **Suangsuda Supasai:** Conceptualization, Methodology, Investigation, Writing - review & editing. **Gene G. Gurkoff:** Writing - review & editing, Supervision. **Jill L. Silverman:** Resources, Writing - review & editing, Supervision. **Pamela J. Lein:** Conceptualization, Writing - review & editing, Supervision, Project administration, Funding acquisition.

Declaration of Competing Interest

The authors declare that they have no known competing financial interests or personal relationships that could have appeared to influence the work reported in this paper.

Acknowledgments

We thank Dr. Suzette Smiley-Jewell (UC Davis CounterACT Center) for her assistance in editing this manuscript.

Funding sources

This work was supported by the Counter ACT Program, National Institutes of Health (NIH) Office of the Director and the National Institute of Neurological Disorders and Stroke (NINDS) [grant number U54 NS079202], and predoctoral fellowships to E.A.G from the NINDS [grant number F31 NS110522], the NIH Initiative for Maximizing Student Development [grant number R25 GM5676520], and the ARCS Foundation. This project used core facilities supported by the UC Davis MIND Institute Intellectual and Developmental Disabilities Research Center (P50 HD103526). The sponsors were not involved in the study design, in the collection, analysis, or interpretation of data, in the writing of the report, or in the decision to submit the paper for publication.

References

Akazawa, C., Shigemoto, R., Bessho, Y., Nakanishi, S., Mizuno, N., 1994. Differential expression of five N-methyl-D-aspartate receptor subunit mRNAs in the cerebellum of developing and adult rats. J. Compar. Neurol. 347 (1), 150–160.

Akman, O., Moshé, S.L., Galanopoulou, A.S., 2014. Sex-specific consequences of early life seizures. Neurobiol. Dis. 72 Pt B 72, 153–166. https://doi.org/10.1016/j.nbd.2014.05.021.

Anagnostaras, S.G., Josselyn, S.A., Frankland, P.W., Silva, A.J., 2000. Computer-assisted behavioral assessment of Pavlovian fear conditioning in mice. Learn. Mem. 7, 58–72. https://doi.org/10.1101/lm.7.1.58.

Barker-Haliski, M., White, H.S., 2015. Glutamatergic Mechanisms Associated with Seizures and Epilepsy. Cold Spring Harb. Perspect. Med. 5, a022863. https://doi.org/10.1101/cshperspect.a022863.

Bell, M.R., 2018. Comparing postnatal development of gonadal hormones and associated social behaviors in rats, mice, and humans. Endocrinology 159, 2596–2613. https://doi.org/10.1210/en.2018-00220.

Berg, E.L., Pedersen, L.R., Pride, M.C., Petkova, S.P., Patten, K.T., Valenzuela, A.E., Wallis, C., Bein, K.J., Wexler, A., Lein, P.J., Silverman, J.L., 2020. Developmental exposure to near roadway pollution produces behavioral phenotypes relevant to neurodevelopmental disorders in juvenile rats. Transl. Psychiatry 10, 289. https://doi.org/10.1038/s41398-020-00978-0.

Bian, C., Zhu, K., Guo, Q., Xiong, Y., Cai, W., Zhang, J., 2012. Sex differences and synchronous development of steroid receptor coactivator-1 and synaptic proteins in the hippocampus of postnatal female and male C57BL/6 mice. Steroids 77 (1-2), 149–156. https://doi.org/10.1016/j.steroids.2011.11.002.

BRUCE, R., 1985. An up-and-down procedure for acute toxicity testing. Fundam. Appl. Toxicol.: Off. J. Soc. Toxicol. 5 (1), 151–157. https://doi.org/10.1016/0272-0590(85)90059-4.

Chen, Y., 2012. Organophosphate-induced brain damage: mechanisms, neuropsychiatric and neurological consequences, and potential therapeutic strategies. Neurotoxicology 33 (3), 391–400. https://doi.org/10.1016/j.neuro.2012.03.011.

Cho, K.O., Lybrand, Z.R., Ito, N., Brulet, R., Tafacory, F., Zhang, L., Good, L., Ure, K., Kernie, S.G., Birnbaum, S.G., Scharfman, H.E., Eisch, A.J., Hsieh, J., 2015. Aberrant hippocampal neurogenesis contributes to epilepsy and associated cognitive decline. Nat. Commun. 6, 6606. https://doi.org/10.1038/ncomms7606.

Chudomel, O., Herman, H., Nair, K., Moshé, S.L., Galanopoulou, A.S., 2009. Age- and gender-related differences in GABAA receptor-mediated postsynaptic currents in GABAergic neurons of the substantia nigra reticulata in the rat. Neuroscience 163 (1), 155–167. https://doi.org/10.1016/j.neuroscience:2009.06.025.

Comfort, N., Re, D.B., 2017. Sex-Specific Neurotoxic Effects of Organophosphate Pesticides Across the Life Course. Curr. Environ. Health Rep. 4 (4), 392–404. https://doi.org/10.1007/s40572-017-0171-y.

Couillard-Despres, S., Winner, B., Schaubeck, S., Aigner, R., Vroemen, M., Weidner, N., Bogdahn, U., Winkler, J., Kuhn, H.G., Aigner, L., 2005. Doublecortin expression levels in adult brain reflect neurogenesis. Eur. J. Neurosci. 21, 1–14. https://doi.org/10.1111/j.1460-9568.2004.03813.x.

Damborsky, J.C., Winzer-Serhan, U.H., 2012. Effects of sex and chronic neonatal nicotine treatment on $Na^{2+}/K^{+}/Cl^{-}$ co-transporter 1, K^{+}/Cl^{-} co-transporter 2, brain-derived neurotrophic factor, NMDA receptor subunit 2A and NMDA receptor subunit 2B mRNA expression in the postnatal rat hippocampus. Neuroscience 225, 105–117. https://doi.org/10.1016/j.neuroscience.2012.09.002.

de Araujo Furtado, M., Rossetti, F., Chanda, S., Yourick, D., 2012. Exposure to nerve agents: From status epilepticus to neuroinflammation, brain damage, neurogenesis and epilepsy. Neuro Toxicol. 33 (6), 1476–1490. https://doi.org/10.1016/j.neuro.2012.09.001.

Deshpande, L.S., Carter, D.S., Blair, R.E., DeLorenzo, R.J., 2010. Development of a prolonged calcium plateau in hippocampal neurons in rats surviving status epilepticus induced by the organophosphate diisopropylfluorophosphate. Toxicol. Sci.: Off. J. Soc. Toxicol. 116, 623–631. https://doi.org/10.1093/toxsci/kfq157.

Ellman, G.L., Courtney, K.D., Andres, V., Featherstone, R.M., 1961. A new and rapid colorimetric determination of acetylcholinesterase activity. Biochem. Pharmacol. 7 (2), 88–95.

Fawcett, W.P., Aracava, Y., Adler, M., Pereira, E.F.R., Albuquerque, E.X., 2009. Acute toxicity of organophosphorus compounds in guinea pigs is sex- and age-dependent and cannot be solely accounted for by acetylcholinesterase inhibition. J. Pharmacol. Exp. Ther. 328 (2), 516–524. https://doi.org/10.1124/jpet.108.146639.

Figueiredo, T.H., Apland, J.P., Braga, M.F.M., Marini, A.M., 2018. Acute and long-term consequences of exposure to organophosphate nerve agents in humans. Epilepsia 59 (Suppl 2), 92–99. https://doi.org/10.1111/epi.14500.

Flannery, B.M., Bruun, D.A., Rowland, D.J., Banks, C.N., Austin, A.T., Kukis, D.L., Li, Y., Ford, B.D., Tancredi, D.J., Silverman, J.L., Cherry, S.R., Lein, P.J., 2016. Persistent neuroinflammation and cognitive impairment in a rat model of acute diisopropylfluorophosphate intoxication. Journal of neuroinflammation 13, 267. https://doi.org/10.1186/s12974-016-0744-y.

Gage, M., Golden, M., Putra, M., Sharma, S., Thippeswamy, T., 2020. Sex as a biological variable in the rat model of diisopropylfluorophosphate-induced long-term neurotoxicity. Ann. N. Y. Acad. Sci. 1479 (1), 44–64. https://doi.org/10.1111/nyas.v1479.110.1111/nyas.14315.

Gao, J., Naughton, S.X., Wulff, H., Singh, V., Beck, W.D., Magrane, J., Thomas, B., Kaidery, N.A., Hernandez, C.M., Terry Jr., A.V., 2016. Diisopropylfluorophosphate Impairs the Transport of Membrane-Bound Organelles in Rat Cortical Axons. J. Pharmacol. Exp. Ther. 356, 645–655. https://doi.org/10.1124/jpet.115.230839.

González-Alzaga, B., Lacasaña, M., Aguilar-Garduño, C., Rodríguez-Barranco, M., Ballester, F., Rebagliato, M., Hernández, A.F., 2014. A systematic review of

neurodevelopmental effects of prenatal and postnatal organophosphate pesticide exposure. Toxicol. Lett. 230 (2), 104–121. https://doi.org/10.1016/j.toxlet.2013.11.019.

González, E.A., Rindy, A.C., Guignet, M.A., Calsbeek, J.J., Bruun, D.A., Dhir, A., Andrew, P., Saito, N., Rowland, D.J., Harvey, D.J., Rogawski, M.A., Lein, P.J., 2020. The chemical convulsant diisopropylfluorophosphate (DFP) causes persistent neuropathology in adult male rats independent of seizure activity. Arch. Toxicol. 94 (6), 2149–2162. https://doi.org/10.1007/s00204-020-02747-w.

Guignet, M., Lein, P.J., 2018. Organophosphates. In: Aschner, M., Costa, L.G. (Eds.), Advances in Neurotoxicology: Role of Inflammation in Environmental Neurotoxicity. Elsevier Ltd., Oxford, UK, pp. 35–79.

Guignet, M., Dhakal, K., Flannery, B.M., Hobson, B.A., Zolkowska, D., Dhir, A., Bruun, D. A., Li, S., Wahab, A., Harvey, D.J., Silverman, J.L., Rogawski, M.A., Lein, P.J., 2020. Persistent behavior deficits, neuroinflammation, and oxidative stress in a rat model of acute organophosphate intoxication. Neurobiol. Dis. 133, 104431. https://doi.org/10.1016/j.nbd.2019.03.019.

Gulinello, M., Mitchell, H.A., Chang, Q., Timothy O'Brien, W., Zhou, Z., Abel, T., Wang, L., Corbin, J.G., Veeraragavan, S., Samaco, R.C., Andrews, N.A., Fagiolini, M., Cole, T.B., Burbacher, T.M., Crawley, J.N., 2019. Rigor and reproducibility in rodent behavioral research. Neurobiol. Learn. Mem. 165, 106780. https://doi.org/10.1016/j.nlm.2018.01.001.

Haley, N., 2018. Remarks at an Emergency UN Security Council Briefing on Chemical Weapons Use by Russia in the United Kingdom. United States Mission to the United Nations.

Hanada, T., 2020. Ionotropic Glutamate Receptors in Epilepsy: A Review Focusing on AMPA and NMDA Receptors. Biomolecules 10, 464. https://doi.org/10.3390/biom10030464.

Heiss, D.R., Zehnder, D.W., Jett, D.A., Platoff, G.E., Yeung, D.T., Brewer, B.N., 2016. Synthesis and Storage Stability of Diisopropylfluorophosphate. J. Chem. 2016, 1–5. https://doi.org/10.1155/2016/3190891.

Hobson, B.A., Rowland, D.J., Siso, S., Guignet, M.A., Harmany, Z.T., Bandara, S., Saito, N., Harvey, D.J., Bruun, D.A., Garbow, J.R., Chaudhari, A.J., Lein, P.J., 2019. TSPO PET Using [18F]PBR111 Reveals Persistent Neuroinflammation Following Acute Diisopropylfluorophosphate Intoxication in the Rat. Toxicol. Sci.: Off. J. Soc. Toxicol.. https://doi.org/10.1093/toxsci/kfz096.

Holst, C.B., Brochner, C.B., Vitting-Seerup, K., Mollgard, K., 2019. Astrogliogenesis in human fetal brain: complex spatiotemporal immunoreactivity patterns of GFAP, S100, AQP4 and YKL-40. J. Anat.. https://doi.org/10.1111/joa.12948.

Hsu, C., Hsieh, Y.L., Yang, R.C., Hsu, H.K., 2000. Blockage of N-methyl-D-aspartate receptors decreases testosterone levels and enhances postnatal neuronal apoptosis in the preoptic area of male rats. Neuroendocrinology 71, 301–307. https://doi.org/10.1159/000054550.

Hung, Y.-W., Yang, D.-I., Huang, P.-Y., Lee, T.-S., Kuo, T.B.J., Yiu, C.-H., Shih, Y.-H., Lin, Y.-Y., 2012. The duration of sustained convulsive seizures determines the pattern of hippocampal neurogenesis and the development of spontaneous epilepsy in rats. Epilepsy Res. 98 (2-3), 206–215. https://doi.org/10.1016/j.eplepsyres.2011.09.015.

Jett, D.A., 1998. Central cholinergic neurobiology. In: Handbook of Developmental Neurotoxicology. Elsevier, pp. 257–274.

Jett, D.A., Spriggs, S.M., 2020. Translational research on chemical nerve agents. Neurobiol. Dis. 133, 104335. https://doi.org/10.1016/j.nbd.2018.11.020.

Jett, D.A., Sibrizzi, C.A., Blain, R.B., Hartman, P.A., Lein, P.J., Taylor, K.W., Rooney, A. A., 2020. A national toxicology program systematic review of the evidence for long-term effects after acute exposure to sarin nerve agent. Crit. Rev. Toxicol. 50 (6), 474–490. https://doi.org/10.1080/10408444.2020.1787330.

Kee, N., Sivalingam, S., Boonstra, R., Wojtowicz, J.M., 2002. The utility of Ki-67 and BrdU as proliferative markers of adult neurogenesis. J. Neurosci. Methods 115 (1), 97–105. https://doi.org/10.1016/S0165-0270(02)00007-9.

Kempermann, G., Song, H., Gage, F.H., 2015. Neurogenesis in the Adult Hippocampus. Cold Spring Harbor Perspect. Biol. 7 (9), a018812. https://doi.org/10.1101/cshperspect.a018812.

Kruger, L., Saporta, S., Swanson, L.W., 1995. Photographic atlas of the rat brain: the cell and fiber architecture illustrated in three planes with stereotaxic coordinates. Cambridge University Press, Cambridge.

Kuruba, R., Wu, X., Reddy, D.S., 2018. Benzodiazepine-refractory status epilepticus, neuroinflammation, and interneuron neurodegeneration after acute organophosphate intoxication. Biochim. et Biophysica Acta (BBA) - Molecular Basis of Disease 1864, 2845–2858. https://doi.org/10.1016/j.bbadis.2018.05.016.

Lazarov, O., Hollands, C., 2016. Hippocampal neurogenesis: Learning to remember. Prog. Neurobiol. 138–140, 1–18. https://doi.org/10.1016/j.pneurobio.2015.12.006.

Li, H., Huguenard, J.R., Fisher, R.S., 2007. Gender and age differences in expression of GABAA receptor subunits in rat somatosensory thalamus and cortex in an absence epilepsy model. Neurobiol. Dis. 25 (3), 623–630. https://doi.org/10.1016/j.nbd.2006.11.004.

Liu, C., Li, Y., Lein, P.J., Ford, B.D., 2012. Spatiotemporal patterns of GFAP upregulation in rat brain following acute intoxication with diisopropylfluorophosphate (DFP). Curr. Neurobiol. 3, 90–97.

McDonough Jr., J.H., Shih, T.M., 1997. Neuropharmacological mechanisms of nerve agent-induced seizure and neuropathology. Neurosci. Biobehav. Rev. 21, 559–579.

Mew, E.J., Padmanathan, P., Konradsen, F., Eddleston, M., Chang, S.S., Phillips, M.R., Gunnell, D., 2017. The global burden of fatal self-poisoning with pesticides 2006–15: Systematic review. J. Affect. Disord. 219, 93–104. https://doi.org/10.1016/j.jad.2017.05.002.

Monyer, H., Burnashev, N., Laurie, D.J., Sakmann, B., Seeburg, P.H., 1994. Developmental and regional expression in the rat brain and functional properties of four NMDA receptors. Neuron 12 (3), 529–540.

Muñoz-Quezada, M.T., Lucero, B.A., Barr, D.B., Steenland, K., Levy, K., Ryan, P.B., Iglesias, V., Alvarado, S., Concha, C., Rojas, E., Vega, C., 2013. Neurodevelopmental effects in children associated with exposure to organophosphate pesticides: A systematic review. Neurotoxicology 39, 158–168. https://doi.org/10.1016/j.neuro.2013.09.003.

OPCW, 2020. OPCW Issues Report on Technical Assistance Requested by Germany. Organisation for the Prohibition of Chemical Weapons,

Pereira, E.F.R., Aracava, Y., DeTolla, L.J., Beecham, E.J., Basinger, G.W., Wakayama, E. J., Albuquerque, E.X., 2014. Animal models that best reproduce the clinical manifestations of human intoxication with organophosphorus compounds. J. Pharmacol. Exp. Ther. 350 (2), 313–321. https://doi.org/10.1124/jpet.114.214932.

Pessah, I.N., Rogawski, M.A., Tancredi, D.J., Wulff, H., Zolkowska, D., Bruun, D.A., Hammock, B.D., Lein, P.J., 2016. Models to identify treatments for the acute and persistent effects of seizure-inducing chemical threat agents. Ann. N. Y. Acad. Sci. 1378, 124–136. https://doi.org/10.1111/nyas.13137.

Phelan, K.D., Shwe, U.T., Williams, D.K., Greenfield, L.J., Zheng, F., 2015. Pilocarpine-induced status epilepticus in mice: A comparison of spectral analysis of electroencephalogram and behavioral grading using the Racine scale. Epilepsy Res. 117, 90–96. https://doi.org/10.1016/j.eplepsyres.2015.09.008.

Pope, C.N., Brimijoin, S., 2018. Cholinesterases and the fine line between poison and remedy. Biochem. Pharmacol. 153, 205–216. https://doi.org/10.1016/j.bcp.2018.01.044.

Potier, S., Sénécal, J., Chabot, J.G., Psarropoulou, C., Descarries, L., 2005. A pentylenetetrazole-induced generalized seizure in early life enhances the efficacy of muscarinic receptor coupling to G-protein in hippocampus and neocortex of adult rat. Eur. J. Neurosci. 21, 1828–1836. https://doi.org/10.1111/j.1460-9568.2005.04026.x.

Pouliot, W., Bealer, S.L., Roach, B., Dudek, F.E., 2016. A rodent model of human organophosphate exposure producing status epilepticus and neuropathology. Neurotoxicology 56, 196–203. https://doi.org/10.1016/j.neuro.2016.08.002.

Putra, M., Sharma, S., Gage, M., Gasser, G., Hinojo-Perez, A., Olson, A., Gregory-Flores, A., Puttachary, S., Wang, C., Anantharam, V., Thippeswamy, T., 2019. Inducible nitric oxide synthase inhibitor, 1400W, mitigates DFP-induced long-term neurotoxicity in the rat model. Neurobiol. Dis. 133, 104443. https://doi.org/10.1016/j.nbd.2019.03.031.

Rauh, V.A., Perera, F.P., Horton, M.K., Whyatt, R.M., Bansal, R., Hao, X., Liu, J., Barr, D. B., Slotkin, T.A., Peterson, B.S., 2012. Brain anomalies in children exposed prenatally to a common organophosphate pesticide. PNAS 109 (20), 7871–7876. https://doi.org/10.1073/pnas.1203396109.

Ravizza, T., Friedman, L.K., Moshé, S.L., Veli´šková, J., 2003. Sex differences in GABA (A)ergic system in rat substantia nigra pars reticulata. Int. J. Dev. Neurosci. : Off. J. Int. Soc. Dev. Neurosci. 21 (5), 245–254. https://doi.org/10.1016/S0736-5748(03)00069-8.

Reddy, S.D., Wu, X., Kuruba, R., Sridhar, V., Reddy, D.S., 2020. Magnetic resonance imaging analysis of long-term neuropathology after exposure to the nerve agent soman: correlation with histopathology and neurological dysfunction. Ann. N. Y. Acad. Sci. 1480 (1), 116–135. https://doi.org/10.1111/nyas.v1480.110.1111/nyas.14431.

Ritz, C., Streibig, J.C., 2005. Bioassay Analysis Using R. 2005 12, 22, 10.18637/jss.v012.i05.

Rojas, A., Ganesh, T., Wang, W., Wang, J., Dingledine, R., 2020. A rat model of organophosphate-induced status epilepticus and the beneficial effects of EP2 receptor inhibition. Neurobiol. Dis. 133,. https://doi.org/10.1016/j.nbd.2019.02.010 104399.

Sagiv, S.K., Bruno, J.L., Baker, J.M., Palzes, V., Kogut, K., Rauch, S., Gunier, R., Mora, A. M., Reiss, A.L., Eskenazi, B., 2019. Prenatal exposure to organophosphate pesticides and functional neuroimaging in adolescents living in proximity to pesticide application. PNAS 116, 18347–18356. https://doi.org/10.1073/pnas.1903940116.

Scharfman, H.E., MacLusky, N.J., 2014. Sex differences in the neurobiology of epilepsy: a preclinical perspective. Neurobiol. Dis. 72 (Pt B), 180–192. https://doi.org/10.1016/j.nbd.2014.07.004.

Schmued, L.C., Stowers, C.C., Scallet, A.C., Xu, L., 2005. Fluoro-Jade C results in ultra high resolution and contrast labeling of degenerating neurons. Brain Res. 1035, 24–31. https://doi.org/10.1016/j.brainres.2004.11.054.

Scholl, E.A., Miller-Smith, S.M., Bealer, S.L., Lehmkuhle, M.J., Ekstrand, J.J., Dudek, F. E., McDonough, J.H., 2018. Age-dependent behaviors, seizure severity and neuronal damage in response to nerve agents or the organophosphate DFP in immature and adult rats. Neurotoxicology 66, 10–21. https://doi.org/10.1016/j.neuro.2018.02.018.

Semple, B.D., Blomgren, K., Gimlin, K., Ferriero, D.M., Noble-Haeusslein, L.J., 2013. Brain development in rodents and humans: Identifying benchmarks of maturation and vulnerability to injury across species. Prog. Neurobiol. 106–107, 1–16. https://doi.org/10.1016/j.pneurobio.2013.04.001.

Siso, S., Hobson, B.A., Harvey, D.J., Bruun, D.A., Rowland, D.J., Garbow, J.R., Lein, P.J., 2017. Editor's Highlight: Spatiotemporal Progression and Remission of Lesions in the Rat Brain Following Acute Intoxication With Diisopropylfluorophosphate. Toxicol. Sci.: Off. J. Soc. Toxicol. 157, 330–341. https://doi.org/10.1093/toxsci/kfx048.

Supasai, S., González, E.A., Rowland, D.J., Hobson, B., Bruun, D.A., Guignet, M.A., Soares, S., Singh, V., Wulff, H., Saito, N., Harvey, D.J., Lein, P.J., 2020. Acute

administration of diazepam or midazolam minimally alters long-term neuropathological effects in the rat brain following acute intoxication with diisopropylfluorophosphate. Eur. J. Pharmacol. 886,. https://doi.org/10.1016/j.ejphar.2020.173538 173538.

Tanaka, K., Graham, S.H., Simon, R.P., 1996. The role of excitatory neurotransmitters in seizure-induced neuronal injury in rats. Brain Res. 737, 59–63. https://doi.org/10.1016/0006-8993(96)00658-0.

Toda, T., Gage, F.H., 2018. Review: adult neurogenesis contributes to hippocampal plasticity. Cell Tissue Res. 373, 693–709. https://doi.org/10.1007/s00441-017-2735-4.

UN, 2017. Report of the Independent International Commission of Inquiry on the Syrian Arab Republic. United Nations General Assembly: Human Rights Council.

Varodayan, F.P., Zhu, X.-J., Cui, X.-N., Porter, B.E., 2009. Seizures increase cell proliferation in the dentate gyrus by shortening progenitor cell-cycle length. Epilepsia 50, 2638–2647. https://doi.org/10.1111/j.1528-1167.2009.02244.x.

Velazco-Cercas, E., Beltran-Parrazal, L., Morgado-Valle, C., López-Meraz, M.L., 2020. Status Epilepticus Increases Cell Proliferation and Neurogenesis in the Developing Rat Cerebellum. Cerebellum (London, England) 19, 48–57. https://doi.org/10.1007/s12311-019-01078-6.

Velíšková, J., Desantis, K.A., 2013. Sex and hormonal influences on seizures and epilepsy. Horm. Behav. 63, 267–277. https://doi.org/10.1016/j.yhbeh.2012.03.018.

Wu, P., Hu, Y., Li, X.J., Cheng, M., Jiang, L., 2019. Sodium valproate suppresses abnormal neurogenesis induced by convulsive status epilepticus. Neural Regener. Res. 14, 480–484. https://doi.org/10.4103/1673-5374.245475.

Yang, F., Wang, J.-C., Han, J.-L., Zhao, G., Jiang, W., 2008. Different effects of mild and severe seizures on hippocampal neurogenesis in adult rats. Hippocampus 18, 460–468. https://doi.org/10.1002/hipo.20409.

Zhang, H., Lin, S., Chen, X., Gu, L., Zhu, X., Zhang, Y., Reyes, K., Wang, B., Jin, K., 2019. The effect of age, sex and strains on the performance and outcome in animal models of stroke. Neurochem. Int. 127, 2–11. https://doi.org/10.1016/j.neuint.2018.10.005.

Zitman, F.M.P., Richter-Levin, G., 2013. Age and sex-dependent differences in activity, plasticity and response to stress in the dentate gyrus. Neuroscience 249, 21–30. https://doi.org/10.1016/j.neuroscience.2013.05.030.